

# Pheromone-regulated Genes Required for Yeast Mating Differentiation

Scott Erdman, Li Lin, Michael Malczynski, and Michael Snyder

Department of Biology, Yale University, New Haven, Connecticut 06520-8103

**Abstract.** Yeast cells mate by an inducible pathway that involves agglutination, mating projection formation, cell fusion, and nuclear fusion. To obtain insight into the mating differentiation of *Saccharomyces cerevisiae*, we carried out a large-scale transposon tagging screen to identify genes whose expression is regulated by mating pheromone. 91,200 transformants containing random *lacZ* insertions were screened for  $\beta$ -galactosidase ( $\beta$ -gal) expression in the presence and absence of  $\alpha$  factor, and 189 strains containing pheromone-regulated *lacZ* insertions were identified. Transposon insertion alleles corresponding to 20 genes that are novel or had not previously been known to be pheromone regulated were examined for effects on the mating process. Mutations in four novel genes, *FIG1*, *FIG2*, *KAR5/FIG3*, and *FIG4* were found to cause mating defects.

Three of the proteins encoded by these genes, Fig1p, Fig2p, and Fig4p, are dispensible for cell polarization in uniform concentrations of mating pheromone, but are required for normal cell polarization in mating mixtures, conditions that involve cell-cell communication. Fig1p and Fig2p are also important for cell fusion and conjugation bridge shape, respectively. The fourth protein, Kar5p/Fig3p, is required for nuclear fusion. Fig1p and Fig2p are likely to act at the cell surface as Fig1:: $\beta$ -gal and Fig2:: $\beta$ -gal fusion proteins localize to the periphery of mating cells. Fig4p is a member of a family of eukaryotic proteins that contain a domain homologous to the yeast Sac1p. Our results indicate that a variety of novel genes are expressed specifically during mating differentiation to mediate proper cell morphogenesis, cell fusion, and other steps of the mating process.

THE yeast mating response is an excellent model system for the study of receptor-activated cell differentiation in eukaryotes. Upon encountering appropriate mating pheromones, haploid yeast cells follow a programmed pattern of cell differentiation in preparation for later events of mating such as cell and nuclear fusion (Cross et al., 1988; Sprague and Thorner, 1992; Kurjan, 1993; Herskowitz, 1995). Vegetative cells exposed to pheromone stop their progression through the cell cycle and undergo polarized cell growth to form a specialized structure termed a mating projection. Polarized mating cells signal one another through their projections, and thereby direct growth to a mutual site of cell contact and fusion. Cell fusion usually occurs at the tips of the projections, forming a conjugation tube or bridge. Nuclear congression and fusion then take place within the conjugation bridge and the zygote enters the vegetative cell cycle, dividing the diploid nucleus between itself and its bud. Although the cytological events of yeast mating have been well described, the molecular components and mechanisms important for

mating cell morphogenesis, cell fusion, and nuclear fusion are not well understood.

At the molecular level, mating differentiation is initiated by the activation of a receptor-coupled signal transduction cascade. Pheromones are bound by the *STE2* and *STE3* gene products, which are seven transmembrane segment receptors located on the surface of *MATa* and *MAT $\alpha$*  cells, respectively. These receptors are coupled to a heterotrimeric G protein complex and a cytoplasmic mitogen-activated protein (MAP)<sup>1</sup> kinase cascade (Sprague and Thorner, 1992). Transduction of the signal by the MAP kinase cascade leads to activation of the transcription factor Ste12p, which, in turn, promotes the transcription of a set of genes involved in mating-specific functions. These functions include cell cycle arrest in G1, polarized morphogenesis, agglutination, cell fusion, karyogamy, and adaptation to the pheromone signal (Sprague and Thorner, 1992).

1. *Abbreviations used in this paper:*  $\beta$ -gal,  $\beta$ -galactosidase; DAPI, 4',6-diamidino-2-phenylindole; DIC, differential interference-contrast microscopy; FIG, factor-induced gene; MAP, mitogen-activated kinase; ORF, open reading frame; PEG, polyethylene glycol; PRE, pheromone response element; SC, synthetic complete medium; TM, transmembrane; TMD, transmembrane domain; YPD, yeast extract/peptone/dextrose medium.

Address all correspondence to Michael Snyder, Dept. of Biology, PO Box 208103, Yale University, New Haven, CT 06520-8103. Tel.: (203) 432-6139. Fax: (203) 432-6161. E-mail: michael.snyder@yale.edu

Many components of the mating MAP kinase cascade, including the Ste12p transcription factor, have also been shown to be required in both haploid and diploid cells for the transition from the normal yeast form of growth to filamentous forms stimulated by nutrient deprivation conditions (Liu et al., 1993; Roberts and Fink, 1994). These filamentous forms of polarized growth and unipolar budding have been proposed to be a mechanism by which cells forage for more favorable nutrient-rich environments (Gimeno et al., 1992; Kron et al., 1994).

The mating projection produced by cells exposed to pheromone serves two important purposes. First, the projection allows the nonmotile yeast cell to extend towards its mate. The position of the mate is perceived through pheromone gradients emanating from mating partners. This perception, or partner selection, is accomplished through the differential activation of mating pheromone receptors on the surface of the mating cell (Jackson and Hartwell, 1990; Jackson et al., 1991; Segall, 1993). Second, growth of the mating projection is an actin-dependent process that has been shown to depend on several proteins that also participate in polarized growth during budding (e.g., Spa2p, Pea2p, Bem1p, Tpm1p, and Cdc42p) (Herskowitz et al., 1995; Pringle et al., 1995; Roemer et al., 1996). Recent studies have demonstrated a physical association between Cdc24p (the GTP exchange factor for Cdc42p), Bem1p, actin, and the heterotrimeric G proteins associated with the pheromone receptors, suggesting a mechanism for linking pheromone pathway activation to localized cell polarization (Leeuw et al., 1995). However, because these interactions are independent of the state of activation of the pheromone pathway, the specific mechanism of polarization to sites of pheromone receptor activation remains obscure (Leeuw et al., 1995; Roemer et al., 1996).

The second role of the mating projection is to concentrate components involved in cell adhesion (agglutinins), signaling (pheromones and pheromone receptors), and fusion (Fus1p and Fus2p) to the area of intended cell contact and fusion. High levels of mating pheromone are required for normal cell fusion, and several proteins that function specifically in these processes ( $\alpha$ -factor,  $\alpha$ -factor, Ste2p, Fus1p, and Fus2p) are all highly localized to projections or their tips (Trueheart and Fink, 1989; Jackson et al., 1991; Sprague and Thorner, 1992; Elion et al., 1995). Many cell polarity genes also function in the cell fusion pathway as indicated by the increase in cell fusion defects observed for mutants in a number of such genes (e.g., *SPA2*, *PEA2*, *BNII*, *RVS161*) (Dorer et al., 1997). These observations suggest that efficient cell fusion is likely to depend on proper cell polarity to affect localization of the signaling and cell fusion components to the projection tip.

In contrast to our extensive knowledge of the components of the mating signal transduction cascade and their interactions, relatively few proteins are known to be specifically involved in the various downstream events of the mating process (Sprague and Thorner, 1992; Brill et al., 1994; Choi et al., 1994; Stevenson et al., 1995). For example, most of the polarity components known to affect mating cell shape and growth also participate in vegetative functions (Herskowitz et al., 1995; Pringle et al., 1995; Roemer et al., 1996). Thus, it is likely that certain mating-specific components remain undescribed that link general po-

larity proteins to specified sites of cell growth during mating. Some of these components would be expected to help direct the growth and shape of the mating projection. Understanding the downstream events of the mating process, including cell polarization, cell fusion, and nuclear fusion, is of general importance to elucidating these processes in higher eukaryotic cells. The limited number of downstream genes currently identified as functioning in these processes suggested that a search for new pheromone-regulated genes might yield additional components of the mating pathway, and thereby help determine the molecular and cellular mechanisms involved in mating cell differentiation.

We describe the results of an extensive screen for pheromone-regulated genes. The screen uses a recently developed method of random transposon tagging of yeast genes to monitor gene expression and investigate mutant phenotypes (Burns et al., 1994). From an initial bank of 189 pheromone-regulated transposon insertions, 45 new pheromone-regulated genes were identified. Among these 45 genes, 30 represent novel genes and 15 encode genes whose expression was previously unknown to be affected by pheromone. Furthermore, we find that a subset of pheromone-induced genes are also induced by conditions of nitrogen deprivation, suggesting a set of target genes is shared between the mating and pseudohyphal pathways. Four novel pheromone-induced genes designated Factor-Induced Gene *FIG1*, *FIG2*, *KAR5/FIG3*, and *FIG4* were determined to be required for different steps of mating cell differentiation, including the control of mating cell polarity, cell fusion, and nuclear fusion.

## Materials and Methods

### Yeast Strains and General Methods

The yeast strains used in this study are listed in Table VIII. All strains are derivatives of Y800 (Burns et al., 1994) and in the S288c background. Y1406, the diploid strain used in the screen, was constructed by transforming strain Y1400 *MATa-cry1 ura3-52 leu2- $\Delta$ 98 his3- $\Delta$ 200 trp1- $\Delta$ 1* with a PCR fragment (Baudin et al., 1993) containing the *BARI* gene, in which the entire protein coding sequence was substituted with the sequence of the *HIS3* gene. The resulting strain, Y1402, was used to construct Y1405 (*MATa-cry1/MATa-CRY1 bar1::HIS3/leu2::HIS3*) through backcrossing. A *MATa-cry1/MATa-cry1* mitotic recombinant Y1406 was selected from Y1405 by growth on plates containing crytoleuorine and then confirmed to be a diploid by transformation of a *MATa* plasmid, sporulation, and tetrad analysis. Y1411, the *MATa bar1* haploid strain used for screening is an ascospore segregant derived in the construction of Y1405. General cloning procedures are described in Sambrook et al. (1989). Yeast media and methods are presented in Rose et al. (1990) and Sherman (1986).

### Identification of Pheromone-regulated Genes

The plate assay for detection of pheromone-induced genes was first optimized using two Y1406 strains: one containing a *cik1::lacZ* fusion carried on a YCp50 plasmid and the other a *FUS1::lacZ* fusion carried on a 2  $\mu$ -based plasmid (Trueheart et al., 1987; Page and Snyder, 1992). Cells were grown on yeast extract/peptone/dextrose medium (YPD) plates and then replicated to two 1-mm filters (Whatman Inc., Clifton, NY). The duplicate filters were incubated for an additional 6 h on YPD medium and then transferred to petri dishes containing 0.8 ml of liquid YPD medium, one of which contained 5  $\mu$ g/ml of  $\alpha$ -factor (Sigma Chemical Co., St. Louis, MO). After incubation at 30°C, the filters containing cells were exposed to chloroform vapors to permeabilize the cells, and then the filters were incu-

bated on plates containing X-gal as described previously (Xie et al., 1993). In initial optimization experiments, cells were incubated for 6, 8, 10, and 12 h at 30°C, and then processed for  $\beta$ -gal activity. Optimal signals were observed using pheromone incubation times of 10–12 h, which were used in screening experiments.

A yeast *lacZ* fusion library (Burns et al., 1994) was transformed into strains Y1406 and Y1411. 55,000 Y1406 and 36,200 Y1411 *Leu*<sup>+</sup> transformants were patched on 90-mm petri plates containing synthetic complete (SC) medium lacking leucine (100 transformants/plate). After growth for 2 or 3 d at 30°C, the cells were replica-plated to two filters and incubated on YPD plates for an additional 6–12 h. Filters were processed as described above and strains containing potential pheromone-regulated fusions were identified. Individual strains were then retested as single colonies to identify strains that contained reproducibly pheromone-regulated fusions. 14% of yeast strains expressed  $\beta$ -gal after vegetative growth for a total of ~13,000 strains. Since there are ~6,500 yeast genes in yeast (Mewes et al., 1997), this corresponds to 2.0 genome equivalents screened. Therefore, 158 out of 189 pheromone-regulated fusions corresponds to 1.7 genome equivalents analyzed.

The yeast sequence adjacent to the *mTn3::lacZ* insertion was determined using plasmid rescue procedures described previously (Burns et al., 1994, 1996). Briefly, either YIp5 or pRSQ plasmids were integrated into the *mTn3* insertion, and the yeast sequences adjacent to *lacZ* were recovered as plasmids in *Escherichia coli*. A primer complementary to the end of the *lacZ* sequence was used to determine the sequences of the yeast DNA adjacent to the *mTn3* insertions. The yeast sequences were compared to those in the GenBank database using the BLAST program (Altschul et al., 1990). These sequences (see Table 1) are accessible in GenBank by a search using keywords Pheromone and the fusion number of interest (e.g., P158). Pheromone response element (PRE) sites were identified by searching sequences using the Fitconsensus program of the UWGCG package (Devereaux et al., 1984) and the sites described in (Kronstad et al., 1987).

### Quantitative $\beta$ -galactosidase ( $\beta$ -gal) Assays

Cells of the indicated strains were grown to midlogarithmic phase ( $OD_{600} = 0.4$ ) in SC medium lacking leucine and then divided into two 10-ml aliquots. To determine pheromone induction levels, cells were treated for 2 h in YPD or YPD + 5  $\mu$ g/ml of  $\alpha$ -factor, after which cell lysates were prepared and  $\beta$ -gal activities were measured. Low nitrogen induction levels were measured by comparison of activities in cell lysates of cells grown for 12 h in SC lacking leucine or SC lacking both leucine and  $(NH_4)_2SO_4$ . Cells were harvested by centrifugation, washed once in Z buffer (60 mM  $Na_2HPO_4$ , 40 mM  $NaH_2PO_4$ , 10 mM KCl, 1 mM  $MgSO_4$ , 50 mM  $\beta$ -mercaptoethanol, pH 7.0) and the cell pellet frozen at 70°C until use. Cells were prepared for lysis by resuspending the frozen cell pellet in 0.5 ml of Z buffer, and followed by the addition of 250  $\mu$ g zymolyase 100T to spheroplast cells (30 min at 30°C). Lysates were made by the addition of ~50  $\mu$ l of glass beads (model G-8772; Sigma Chemical Co.), 15  $\mu$ l of 100 mM PMSF, 7.5  $\mu$ l of 20% SDS, and 25  $\mu$ l of chloroform followed by vortexing for 2 min. Assays of  $\beta$ -gal activity were performed by the addition of 200  $\mu$ l of the lysate to 0.8 ml of Z buffer and 200  $\mu$ l of 4 mg/ml *O*-nitrophenol- $\beta$ -D-galactopyranoside. Reactions were stopped with 250  $\mu$ l of 2 M  $Na_2CO_3$ , and then the activities were determined as a function of sample absorbance at 420nm, reaction time, and protein concentration (determined by Bradford assays).

### Disruption of *FIG1*, *FIG2*, *KAR5/FIG3*, and *FIG4*

Complete deletions of the *FIG1*, *FIG2*, *KAR5/FIG3*, and *FIG4* genes were made using a PCR disruption procedure (Baudin et al., 1993). Oligonucleotides containing the 55 bp immediately upstream of the ATG and downstream of the termination codon of each gene were synthesized with ends corresponding to sequences A and B below, respectively. Sequences A and B are complementary to regions that flank the *URA3* gene of pRS316 (Sikorski and Hieter, 1989). *URA3* fragments containing *FIG* flanking sequences were amplified by PCR and then transformed into the diploid strain Y800. Strains containing the correct substitution at the genomic locus were identified by PCR analysis. The resulting heterozygotes were sporulated and then haploid segregants were analyzed for vegetative growth and mating defects. Growth rates of all *fig* $\Delta$  strains were identical to those of wild-type strains at 16, 30 and 37°C. (A) 5'-...AGGCG-CGTTTCGGTGATGACGGTG; (B) 5'-...AGGGTGATGGTTCACG-TAGTGGGC.

### Localization of *Fig1::* $\beta$ -gal and *Fig2::* $\beta$ -gal Proteins

*MATa* cells of the indicated strains were grown to midlogarithmic phase ( $OD_{600} = 0.3$ – $0.4$ ) in YPD, divided into 10-ml cultures, and then incubated for 2 h in either the presence or absence of 5  $\mu$ g/ml  $\alpha$ -factor. Cells were harvested, fixed, and processed for immunofluorescence as described (Gehring and Snyder, 1990; Pringle et al., 1991). To visualize  $\beta$ -gal fusion proteins, a rabbit anti- $\beta$ -gal primary antibody (Cappel Laboratories, Malvern, PA) was used at 1:12, followed by a CY3-conjugated sheep anti-rabbit secondary antibody (Sigma Chemical Co.) used at 1:200. All antibodies were preadsorbed against fixed and spheroplasted yeast cells before use.

### Analysis of Yeast Mating Defects

Haploid strains containing the *lacZ* fusion insertion mutations were recovered by transforming the heterozygous *MATa/MATa* diploid strain with a YCp50 plasmid containing the *MATa* gene (gift of F. Cross, Rockefeller University, NY) followed by sporulation of the transformants. *MATa* segregants containing the transposon insertion mutation were recovered and mated to strain Y1402. *MATa* and *MATa* segregants were then obtained and tested for mating defects. Unilateral matings were carried out between *MATa* mutant strains and strain Y1408. Bilateral matings were performed between *MATa* and *MATa* segregants carrying either the same transposon insertion mutation or deletion. Diploids from the matings were selected on SC medium lacking histidine and tryptophan. Liquid mating reactions were carried out as described in Gehring and Snyder (1990); agents such as polyethylene glycol (PEG)<sub>3350</sub>, EGTA,  $\alpha$ -factor, and polymyxin-B sulfate (Sigma Chemical Co.) were added to the tester strains immediately before addition of the strains whose mating efficiency was being measured. Relative mating efficiencies given in Table IV represent the mean of two separate assays and are normalized to wild-type levels (1.0% diploid formation). Filter mating assays were performed as described in Sprague (1991). Under these conditions, the wild-type frequency of diploid formation was  $51.8 \pm 1.3\%$ ; similar relative frequencies of mating were observed for *fig1* $\Delta$  and *fig4* $\Delta$  strains. *fig2* $\Delta$  strains exhibit a slight (1.5 $\times$ ) increase in cell number/ $OD_{600}$  of cells. However, this cannot account for the increase in mating efficiency of *fig2* $\Delta$  mutants in unilateral and bilateral matings under liquid conditions: experiments in which the density of cells in wild-type control matings similarly increased, or *fig2* $\Delta$  cells decreased, did not show comparable increases in mating efficiency (data not shown).

Projection formation was analyzed by two methods. To assess projection formation in the presence of isotropic pheromone, cultures of mutant strains were grown to  $OD_{600} = 0.3$ – $0.5$  and  $\alpha$ -factor was then added to final concentrations of 0.5, 1.0, 2.5, and 5  $\mu$ g/ml. Second, after incubation for 1, 2, and 4 h, cell morphologies were examined by phase-contrast microscopy. Under these conditions in our strain background, cell cycle arrest is observed at the lowest pheromone concentration and polarized cells with broad projections are formed at intermediate concentrations, whereas sharp mating projections are formed at the highest concentration.

Polarized projection formation and zygote morphologies were also analyzed for the *fig* $\Delta$  strains by quantitation of different cell types present in mating mixes. For these assays, cultures of mutant strains were grown to  $OD_{600} = 0.5$ , and then 2 ml of each were mixed and pelleted by low-speed centrifugation. Mating cells were then resuspended in 5 ml of fresh YPAD and allowed to mate for either 8 h at 30°C or 16 h at 16°C without shaking. After incubation, cells were fixed by the addition of formaldehyde to a final concentration of 3.7% for  $\geq 1$  h, sonicated briefly to disperse cells and zygotes, and then washed and stored in 1 $\times$  PBS, 1 M sorbitol. Cell mixtures were prepared for microscopy by pelleting an aliquot of the mating mix and resuspending in mounting solution containing 4',6-diamidino-2-phenylindole (DAPI) (70% glycerol, 30% PBS, 2% wt/vol *n*-propyl gallate, 0.0225  $\mu$ g/ml DAPI). The scoring of cell type (round, small, or large polarized) was done by placing an aliquot of the fixed cells in a haemocytometer to facilitate counting. Round cells were scored as unpolarized; polarized cells contained projections and were counted as small–medium (with an overall length less than that of a typical zygote), or large (equal to or larger in length than a typical zygote). Quantitation of projection tip shape was determined by scoring medium to large cells, as these cells have longer projections, the shape of which (pointed or blunt) are most clearly differentiated. When indicated, staining of cytoplasmic membranes and lipids was done after fixation by addition of FM4-64 (Molecular Probes, Inc., Eugene, OR) to 33  $\mu$ M final concentration, followed by incubation of the cells on ice for 30 min. Cells were then washed once in 1 $\times$  PBS, 1 M sorbitol before resuspending in mounting solution containing DAPI. Un-

der these conditions (i.e., in formaldehyde-fixed cells) FM4-64 uniformly stains the cytoplasm and nucleus, but is absent from cell wall material as judged by both the reduced diameter of the staining region relative to the cell outline (as viewed by differential interference-contrast microscopy [DIC] optics), and by the absence of staining at sites of cytokinesis in budded cells. Measurements of zygotes comparing fusion bridge width to the mean width of the parental pair were performed using an intraocular micrometer at a magnification of 1600 $\times$ . 50 zygotes were measured for each strain.

Electron microscopy of thin sections through zygotes was as described in Byers and Goetsch (1975), with the following differences. Zygotes were prepared by mating cells as described above; they were pelleted, washed once in 2 ml 0.1 M cacodylate buffer, pH 7.4, and then fixed in 0.1 M cacodylate, pH 7.4, containing fresh 3% glutaraldehyde for 30 min at room temperature. Cells and zygotes were then washed once in 0.1 M cacodylate buffer and then stained with 4%  $\text{KMnO}_4$ , followed by dehydration through a series of ethanol washes, and then embedded in LR-White acrylic resin (Polysciences Inc., Warrington, PA) before sectioning. Sections were stained with uranyl acetate and lead citrate and then viewed on an electron microscope (model EM-109; Carl Zeiss, Inc., Thornwood, NY) at magnifications of 8–40,000 $\times$ . Pheromone sensitivity of the different strains was assayed by the halo method using strains Y1450 and Y1451 (Sprague, 1991).

## Results

### Isolation of Pheromone-regulated Genes

To identify genes specifically regulated during yeast mating, a random *lacZ* insertional mutagenesis scheme was used. This method uses a library of yeast DNA fragments containing mini-Tn3::*lacZ*::*LEU2* insertions (Burns et al., 1994). The *lacZ* gene lies near one end of the insertion and lacks an ATG initiator methionine codon; therefore, expression in yeast is primarily expected to occur because of in-frame insertion into yeast genes to produce yeast protein:: $\beta$ -gal fusions. The library was introduced into either a diploid *MATa/MATa leu2 $\Delta$ /leu2 $\Delta$  bar1 $\Delta$ /bar1 $\Delta$*  or a haploid *MATa leu2 $\Delta$  bar1 $\Delta$*  yeast strain, and then transformants that exhibited enhanced or reduced expression of  $\beta$ -gal in the presence of the  $\alpha$ -factor mating pheromone were identified. The use of a diploid strain allows for the isolation of pheromone-regulated genes that are essential for vegetative growth, whereas the use of strains that lack the Bar1 protease degrades  $\alpha$ -factor increases the responsiveness of the cells to pheromone under our screening conditions. To facilitate screening large numbers of transformants, an X-gal plate assay for identifying pheromone regulated  $\beta$ -gal fusions was developed and then optimized using two yeast strains expressing  $\beta$ -gal fusions with known pheromone-induced proteins, *Fus1p* and *Cik1p* (refer to Materials and Methods; Trueheart et al., 1987; Page and Snyder, 1992).

55,000 transformants of a diploid strain and 36,200 transformants of a haploid strain were screened for  $\beta$ -gal expression in the presence and absence of  $\alpha$ -factor. 186 strains were identified that reproducibly exhibited increased  $\beta$ -gal activity after pheromone treatment; three strains displayed decreased activity after treatment. Examples of the pheromone regulated- $\beta$ -gal expression levels observed for *lacZ* fusions in the four novel *FIG* genes further characterized in this study, and an example of the class of pheromone-repressed genes are presented in Fig. 1.

To determine the identity of the pheromone-regulated yeast genes producing the  $\beta$ -gal fusion proteins, the yeast genomic DNA adjacent to the *lacZ* insertions was plasmid-rescued into *E. coli* and then sequenced for 158 fusion

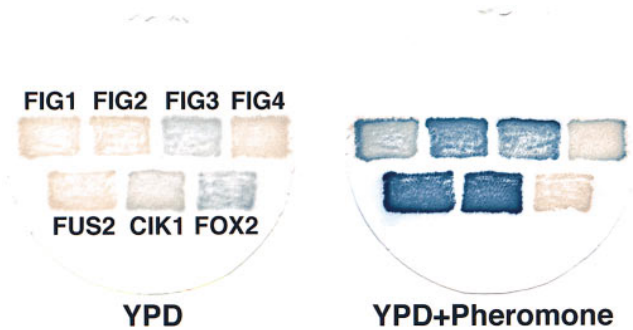


**Figure 1.** Examples of pheromone-regulated *lacZ* fusions. Seven yeast strains containing the *lacZ* fusions indicated were incubated in YPD medium in either the absence (left) or presence (right) of pheromone for 12 h. Examples are shown of strains with fusions in genes whose expression is dependent upon mating pheromone (*FUS2*, *FIG1*, *FIG2*, and *FIG4*), enhanced by pheromone (*CIK1*, *KAR5/FIG3*), or repressed by pheromone (*FOX2*).

strains (Burns et al., 1994). A summary of these results and the relative levels of vegetative and pheromone-induced (or -repressed) expression for the different pheromone-regulated genes identified in this study is presented in Table I. Based on the combined criteria of expression pattern and sequence identity, the fusions occur in genes that can be classified into five major categories: (a) known pheromone-induced genes; (b) previously characterized genes not reported to be induced by pheromone; (c) novel pheromone-induced genes; (d) pheromone-repressed genes; and (e) pheromone- and nitrogen-regulated genes.

Comparison of the number of genes identified by our screen to the total number of reported pheromone-induced genes ( $\sim 22$ , Sprague and Thorner, 1992; Table I), along with the observation that many genes are represented by only one or two transposon fusions, indicates that our screen is not yet saturated. However, many genes are represented by multiple independent insertions. Extrapolating from the number of different genes identified, 54, and the 1.7 genome equivalents screened and analyzed (refer to Materials and Methods), we estimate there are  $\sim 67$  different pheromone-regulated genes in yeast. This number is probably an underestimate because our transposon mutagenesis procedures have certain biases as shown by the overrepresentation of fusions to *SPO11* and *HOG1* (Burns et al., 1994). A larger and probably more accurate figure of 132 genes is obtained if we extrapolate from the number of pheromone-induced genes identified in our screen, nine, with those already known. Thus, we conclude there are  $\sim 67$ –132 pheromone-induced genes in yeast, thereby comprising 1–2% of all yeast genes.

### Several Types of Genes Respond to Mating Pheromone

65 insertions reside in nine known pheromone-induced genes including *STE6*, *FUS2*, *PCL2*, *CIK1*, *AFR1*, *KAR4*, and Ty elements (see Table I for references). Ty1, Ty2, and Ty3 were previously known to be pheromone-induced (Boeke and Sandmeyer, 1991; Sprague and Thorner, 1992; Kurihara et al., 1996); our study indicates that the expression of Ty5 elements is also induced. Ty elements and their

long terminal repeats (LTRs) are abundant in the genome (Olson, 1991), and comprise a large fraction (50 out of 158) of the pheromone-induced fusions identified in this screen. Additionally, some of the genes identified in this study are located adjacent to known pheromone-induced genes (see Table I). Examples include fusion P313B, which lies in an open reading frame (ORF) adjacent to *AFRI*, and the fusions in *YFL027c* (P28) and the *HOG1* gene (P423A), which lie next to *STE2* and a *Ty* LTR delta sequence, respectively. It is likely that the nearby regulatory sequences affect the expression of these genes as documented previously for *Ty* elements (Van Arsdell et al., 1987; Company et al., 1988). Some of these cross-regulated genes may also perform functions in the mating pathway.

In addition to known pheromone-induced genes, many genes (13) had been identified previously, but were not known to be pheromone-induced (Table I B). These include *SPO11*, *HOG1*, *CKI3/YCK3*, and *RVS161*. *SPO11* is a sporulation-induced gene required in the early steps of meiosis. *HOG1* is a MAP kinase homologue that regulates the osmotic stress response (Brewster et al., 1993). *CKI3/YCK3* is a homologue of the yeast casein kinase I-related genes *YCK1*, *YCK2*, and *HRR25*, and has recently been identified as a high copy suppressor of *gcs1* mutants, which are defective in exit from stationary phase (Wang et al., 1996). *RVS161*, previously characterized as playing a role in actin cytoskeletal functions and cell polarity, has recently been described as important for efficient cell fusion and mating under certain conditions (Crouzet et al., 1991; Dorer et al., 1997). The induced expression of these genes during pheromone response suggests that many of these genes may function in the mating process.

A surprising subset of the pheromone-induced genes identified in this study include genes which are known, or can be expected to participate in pseudohyphal growth and/or in nitrogen metabolism, a determinant of pseudohyphal growth (Gimeno et al., 1992; Ljungdahl et al., 1992). These genes include *PHD1*, *YFL056c*, *GAPI*, *AMD1*, *DURI,2*, and potentially *YGR111w*. *PHD1* was originally isolated as a gene that, when present in multiple copies, promotes pseudohyphal growth (Gimeno and Fink, 1994). *YFL056c* encodes a protein with 57% amino acid identity over the first 174 of its 212 residues to an aryl alcohol dehydrogenase from the white-rot fungus *Phanerochaete chrysosporium*. In that organism, the gene is induced by nitrogen starvation conditions, and its product is implicated in lignin degradation (Reiser et al., 1994). The degradation of lignins, an important constituent of plant cell walls, facilitates fungal invasion into host plant tissues. *GAPI* and *AMD1* encode a general amino acid permease and *AMD1* encodes a putative amidase. *YGR111w* encodes a probable lysine N6-acetyltransferase, an enzyme involved in the degradation of lysine. *DURI,2* encodes a urea amidolyase that converts urea to ammonia. The functions of these last four genes are likely to permit the efficient use of alternative nitrogen sources such as those provided by amino acids. *PHD1*, *GAPI*, *AMD1*, and *DURI,2* (Table I E) are each induced by nitrogen starvation (Table III), as has been shown previously for *DURI,2* and *GAPI* (Jau-niaux and Grenson, 1990; Stanbrough and Magasanik, 1995).

Another class of pheromone-regulated genes display decreased expression in pheromone-treated cells. The three

pheromone-repressed genes we identified include: *PHO81*, *FOX2*, and a novel gene, *QORI* (refer to Fig. 1 for the pheromone-dependent repression of *FOX2* expression). *PHO81* encodes a repressor of the Pho85 CDK-G1 kinase complex (Ogawa et al., 1995), *FOX2* functions in peroxisome biogenesis (Kunau and Hartig, 1992), and *QORI* has strong similarity to quinone oxidoreductases, suggesting a function in oxidative respiration in mitochondria. The relatively limited number of pheromone-repressed genes identified may be the result of the long half-life (~20 h) of  $\beta$ -gal in yeast (Bachmair et al., 1992); this could make many pheromone-repressed genes difficult to identify in the 12-h pheromone incubation used in our screen. Surprisingly, the *FOX2* and *QORI*  $\beta$ -gal fusions are not in-frame. However, it is likely that these out-of-frame fusions reflect the normal regulation patterns of these genes. In a separate study, we have prepared an in-frame fusion in the *QORI* gene (Minehart, S., S. Erdman, and M. Snyder, unpublished data). Although the absolute levels of expression for the original out-of-frame fusion strain were lower, as expected, both the in- and out-of-frame fusions exhibited similar relative levels and kinetics of  $\beta$ -gal induction (expression of *QORI* is induced by carbon source changes at the diauxic shift) and pheromone repression. Interestingly, each of the pheromone-repressed genes is likely to be subject to glucose repression; possible mechanisms to explain their regulation by the pheromone pathway are presented in the Discussion.

A large number of novel genes was also identified, and further characterization of four of these genes, *FIG1-4*, is presented below. Some novel genes encode proteins that have homologues in higher eukaryotes, whereas others are predicted to encode proteins that lack extensive homology to other known proteins in the databases (Table I C). Nonetheless, many of the unique proteins have distinctive sequence features. For example, many of the novel pheromone-regulated proteins contain regions predicting their insertion into, or association with, cellular membranes (examples include Fig1p, Fig2p, Yar027wp, and Ypl156cp).

Finally, in several cases the *lacZ* fusion resided either in short ORFs, out-of-frame, reverse orientation, or in regions flanking genes (although most fusions were found to be in-frame with ORFs). These results indicate that sequences in addition to long ORFs can be expressed as protein in vivo, and are corroborated both by our previous study that found that short ORFs outside of predicted coding sequences are often expressed, and by recent analyses of the yeast transcriptome using SAGE techniques (Burns et al., 1994; Velculescu et al., 1997). For two genes, *FUS2* and *GAPI*, out-of-frame fusions were found in addition to several in-frame fusions. For both genes, in- and out-of-frame fusions were regulated similarly. Many of the insertions obtained in the *HOG1* region are either out-of-frame, in reverse orientation, or in flanking regions; nonetheless, all exhibit similar levels of pheromone induction consistent with responses to the same regulatory elements in each case. Thus, we presume that in many, if not most, cases, the regulation that is observed for any particular *lacZ* fusion reflects the expression of the transcript for the ORF into which the *lacZ* is inserted, an interpretation supported by our studies with *QORI* insertions. One

Table I. Summary of Pheromone-regulated Genes

Strain # <sup>‡</sup>	Fusions <sup>§</sup>	Gene	Function/comments	Codon/total <sup>  </sup>	Veg. exp. <sup>¶</sup>	Pher. exp. <sup>¶</sup>	Phenotypes <sup>**</sup>	Reference
A. Known pheromone-induced genes								
P374A, P34B-1, P253B, P260B, P105A-2, ...	26	<i>Ty1, Ty2</i>	Transposable elements; fusions in both <i>TyA</i> and <i>TyB</i> were identified	163/ <i>TyA</i> , 245/ <i>TyA</i> , 335*/ <i>TyA</i> , 633/ <i>TyB</i> , 719/ <i>TyB</i>	–	++++	Not tested	Boeke and Sandmeyer (1991)
P5A, P17A, P50A-2, P56B, P108A, ...	22	<i>Ty3/Sigma</i>	Transposable element	Not mapped	–	++++	Not tested	Boeke and Sandmeyer (1991)
P103A, P105A-1, P161A, P225A, P606-A, P606-B, P643	7	<i>FUS2</i>	Cell fusion	86/617, 343/617, 343/617, 327/617, 263*/617, 273/617	–	++++	Not tested	Elion et al. (1995)
P342A, P354B-2, P569A, P695A, P806	5	<i>PCL2</i>	Pho85 cyclin	2/332, 181/332, 2/332, 2/332, 2/332	–	+	None	Measday et al. (1994)
P6C	1	<i>AFR1</i>	Polar growth, adaptation	159/620	++	+++	Not tested	Konopka (1993)
P763	1	<i>KAR4/YCL055w</i>	Karyogamy	180/336	++	++++	Not tested	Kurihara et al. (1996)
P524B	1	<i>CIK1</i>	Kar3 microtubule motor component	537/594	+	+++	Not tested	Page and Snyder (1992)
P372B	1	<i>STE6</i>	Mating factor transporter	400/1290	++	+++	Not tested	Kuchler et al. (1989)
P129B	1	<i>3'to GPA1</i>	G protein, signaling	*	+	++	Not tested	Dietzel and Kurjan (1987); Miyajima et al. (1987)
B. Previously characterized genes not known to be pheromone regulated								
P269B, P398A, P306A, P357A, P436A-2, ...	19	<i>SPO11</i>	Meiosis, recombination	50/398, 68/398, 175/398, 300/398, 322/398	+++	++++	Not tested	Atcheson et al. (1987)
P50A-1, P59A, P61A, P97B, P105B, ...	10	<i>HOG1 region</i>	Osmotic stress response	*	–	+++	Not tested	Brewster et al. (1993)
P27B, P145B, P209B	3	<i>28S rRNA</i>	Ribosomal RNA	*	++	+++	Not tested	Valenzuela et al. (1977)
P177A, P641	2	<i>Ty5</i>	Transposable element LTR; P177 adjacent to element but not in ORF; P641 lies between <i>YHLO48w</i> and 231-bp <i>Ty5</i> LTR	*	–	++++	Not tested	Voytas and Boeke (1992)
P431B, P523C	2	<i>RVS161</i>	Actin cytoskeleton	54/265, 86/265	++	+++	None	Crouzet et al. (1992)
P500A-2	1	<i>YCK3/CK13</i>	Casein kinase III subunit	504/525	–	++	None	Stanford Genomic Database
P33B	1	<i>PMR2</i>	Plasma membrane Na <sup>+</sup> Ion pump	1020/1092	–	±	Not tested	Wieland, J. et al. (1995)
P157B	1	<i>RAP1 region</i>	Chromatin/telomere function; fusion on opposite strand	80/101	+++	++++	Not tested	Shore and Nasmyth (1987)
P86B	1	<i>TOP2</i>	Topoisomerase	1181/1429	+++	++++	Not tested	Giaever et al. (1986)
P7A	1	<i>YL8B</i>	Ribosomal protein YL8B	144/244	–	+	Not tested	Mizuta et al. (1995)
C. Novel pheromone-regulated genes								
P299A, P315A, P452A, P487A, P796, P808	6	<i>YSC8010 region</i>	All fusions lie in small ORF between YM8010.05 and YM8010.06	26/87, 16*/87, 72/87, 7*/87, 72/87, 26/87	–	+++	Not tested	
P403A-2, P332B, P221B-2, P358A	4	<i>FIG4/YNL325c</i>	Required for efficient mating, <i>SAC1</i> homology domain	536/879, 536*/879, 553/879, 604/879	+	++	None	

continued

Table I. (continued)

Strain # <sup>‡</sup>	Fu- sions <sup>§</sup>	Gene	Function/comments	Codon/total <sup>  </sup>	Veg. exp. <sup>¶</sup>	Pher. exp. <sup>¶</sup>	Phenotypes**	Reference
P28A, P787	2	<i>YFL027c</i>	ORF divergent from <i>STE2</i>	163/498, 50/498	–	+++	None	Kurihara et al. (1994), this study
P726A, P900	2	<i>KAR5/</i> <i>FIG3</i>	Required for efficient mating, extensive coiled-coil domain	258/504, 258/504	–	+++	Karyogamy defect	
P158A	1	<i>FIG1/</i> <i>YBR040w</i>	Required for efficient mating, 4 TM domains	101/298	–	++	EGTA sensitive for mating	This study
P294A	1	<i>FIG2/</i> <i>YCR089w</i>	Required for efficient mating, signal peptide/GPI anchor	140/1609	–	+++	Cold sensi- tive for mating	This study
P258B	1	<i>YAR027w</i>	Ycr7p homology, two predicted transmembrane domains, Sigma element upstream	50/235	++	+++	None	
P290A-2	1	<i>YPL156c</i>	Predicted transmembrane domain	67*/284	+	++	None	
P403A-1	1	<i>YER188w</i>		98/239	–	±	None	
P411B-1	1	<i>ADP1/</i> <i>YCR011c</i>	Predicted member of ABC transporter superfamily	874/1049	+	++	None	
P9B	1	<i>YGR111w</i>	Probable lysine degradation enzyme, similarity to lysine N6-acetyl-transferases	309/400	±	+	Not tested	
P510B	1	<i>YIL083c</i>	Adjacent to Sigma element	133/365	+	+ / ++	Not tested	
P569B	1	<i>YNL033w</i>		180/284	–	+	Not tested	
P50B	1	<i>YKR090w</i> <i>region</i>	Short ORF on opposite strand from <i>YKR090w</i> , adjacent fusion found in <i>YKR091w</i>	32/39	–	++	Not tested	
P353A	1	<i>YKR091w</i> <i>region</i>		*	–	+	Not tested	
P313B	1	<i>AFR1</i> <i>region</i>	ORF is divergent to <i>AFR1</i>	15/79	++	+++	Not tested	
P870	1	<i>28S rRNA</i> <i>3' region</i>	Short ORF	15/25	–	++	Not tested	
P390A-2	1	<i>YNL146w</i>	Short ORF, divergent from <i>MFA2</i>	14*/100	±	++	None	
P359A	1	<i>ALK1/</i> <i>YGL021w</i> <i>region</i>	Fusion in short ORF	18/43	+	+++	None	
P346B	1	<i>YKR106w</i> <i>region</i>	Short ORF	2/20	–	++	Not tested	
P681	1	<i>YHR164c-</i> <i>YHR165c</i> <i>region</i>	Short ORF	9/17	++	+++	Not tested	
P914	1	<i>TIF5-</i> <i>YPR039C</i> <i>region</i>	Short ORF	11/12	–	++	Not tested	
P160A, P187A	2	<i>YNR062c-</i> <i>YNR063w</i> <i>region</i>	Identical insertions	*	+	++	None	
P28B-2	1	<i>YSCP9584:</i> <i>P9584.4</i>	Large cluster of <i>Ty</i> and <i>Delta</i> elements 1,673-bp 3' to indicated ORF	*	++	+++	None	
P356B	1	<i>CDC91</i> <i>region</i>	Downstream of <i>CDC91</i>	*	+	+ / ++	Not tested	
P430B	1	<i>YLR057w</i>	Within <i>YLR057w</i> , not in frame	*	–	++	Not tested	
P439B	1	<i>CHRXV</i>	Between ORFs PID:g600477 and PID:g600478	*	+++	+++ / ++++	Not tested	
P482B	1	<i>YNR069c-YNR-</i> <i>070w region</i>		*	±	+	None	
D. Pheromone-repressed genes								
P205B	1	<i>PHO81</i>	Negative regulator of PCL –PHO85 complexes	707/1177	++	+	None	Ogawa et al. (1993)

continued

Table I. (continued)

Strain # <sup>‡</sup>	Fusions <sup>§</sup>	Gene	Function/comments	Codon/total <sup>  </sup>	Veg. exp. <sup>¶</sup>	Pher. exp <sup>¶</sup>	Phenotypes <sup>**</sup>	Reference
P591	1	<i>FOX2</i>	Peroxisome biogenesis, fusion located at 44-bp upstream of <i>FOX2</i> ATG	*	++	±	Not tested	Hiltunen et al. (1992)
P323B	1	<i>QOR1</i>	Predicted mitochondrial quinone oxidoreductase, fusion located within coding sequence, but not in frame	*	+++	++	Not tested	
E. Pheromone and nitrogen-regulated genes <sup>**</sup>								
P2B, P33A	2	<i>PHD1</i>	Promoter of pseudohyphal growth	159/367, 308/367	++	+++	None	Gimeno and Fink (1994)
P274A, P319B-2, P520A, P534C	4	<i>GPA1</i>	General amino acid permease, P319B-2 out of frame at indicated codon	421/601, 392*/601, 466/601, 595/601	++	++++	Not tested	Jauniaux and Grenson (1990)
P809, P820	2	<i>DUR1,2</i>	Urea amidolyase	83/1835	±	++	Not tested	Genbauffe and Cooper (1991)
P713	1	<i>AMD1</i>	Putative amidase	173/549	+	++	Not tested	Chang and Abelson (1990)
P104A	1	<i>YFL056c</i>	Aryl alcohol dehydrogenase homolog	72/212	++	+++	None	Reiser et al. (1994)

<sup>‡</sup>In cases where there are more than seven fusions, five representative fusions were selected for inclusion.

<sup>§</sup>Represents total number of fusions obtained in the screen, independent and non independent.

<sup>||</sup>Fusions that either lie out of frame within or outside of open reading frames are denoted by \*, for the case of *GPA1* the fusion lies in a short ORF, 50 amino acids, and was assigned to the nearest large ORF.

<sup>¶</sup>Based on qualitative X-gal plate assays as depicted in Fig. 1; expression levels range from (-) not detectably expressed to (++++) very strongly expressed.

<sup>\*\*</sup>Mating phenotypes examined in this study as described in Materials and Methods.

<sup>\*\*</sup>A subset of the fusions as described in the text were examined by qualitative X-gal plate assays for induction by low nitrogen conditions. Low nitrogen induction of this group of fusions was confirmed by quantitative  $\beta$ -gal assays and/or previous studies (see text).

mechanism to account for the expression of out-of-frame fusions is translational frameshifting.

### Pheromone-regulated Gene Expression

Based on the results of quantitative  $\beta$ -gal assays presented in Table II, the levels of induced expression upon pheromone treatment are  $\sim 1.3$ - $\rightarrow$ 700-fold for most of the pheromone-induced fusions. In cases where these levels have been measured, the figures reported here agree closely with those found previously (e.g., *FUS2* and *CIK1*; Page and Snyder, 1992; Elion et al., 1995).

An upstream regulatory element termed the PRE has been identified as mediating the pheromone-induced transcription of a number of genes involved in the mating response (e.g., *FUS2*, *CSH1*, *MFA2*, *STE6*, *STE2*, *BARI*, *Ty* elements and *CIK1*) (Van Arsdell et al., 1987). These sequences represent potential binding sites for Ste12p, the transcription factor that mediates pheromone-induced transcription, and are generally found upstream of pheromone-induced protein coding sequences (Kronstad et al., 1987; Errede and Ammerer, 1989; Page and Snyder, 1992). We searched the regions immediately upstream of the four novel *FIG* genes characterized in this study and found sequences matching the PRE consensus (Fig. 2). Since several of these genes are pheromone dependent for their expression yet contain only PRE sites that differ from the consensus, these results indicate that variant PRE sites are likely to be important for Ste12p-dependent regulation of some genes (e.g., *FIG1* and *FIG4*, Fig. 2). An additional

search for Mcm1p binding sites, which can be found near PRE sites of a subset of pheromone-induced genes such as *FUS1* (Herskowitz et al., 1992), failed to identify sequences in the upstream regions of the *FIG1-4* genes closely matching the consensus binding site.

Mating pheromone treatment of cells causes cell cycle arrest in G1, and it has been proposed that this arrest may influence the expression of some genes that would be indirectly controlled by activation of the mating pathway (Stetler and Thorner, 1984; Price et al., 1991). We tested whether the pheromone-induced expression of the four *FIG* genes characterized in the present study is a consequence of direct or indirect regulation by the pheromone-response pathway. *MATa* strains carrying *lacZ* fusions of the four *FIG* genes were crossed to a *MAT $\alpha$*  *cdc28-1* strain, and *MATa* *cdc28-1* *fig::lacZ* progeny were tested for induction of gene expression after cell cycle arrest in the absence of mating pheromone treatment (*cdc28-1* strains shifted to the restrictive temperature arrest in G1). No increase in gene expression was observed for any of the four genes in the absence of pheromone treatment, nor was any expression observed in *a/a* cells (data not shown). In addition, mating-induced expression of the four genes was observed in both *a* and  $\alpha$  cell types as monitored by the mating of strains of either cell type carrying *lacZ* fusions in these genes to yeast strains of the opposite mating type. These data, combined with the presence of upstream sites similar to the PRE consensus sequence in the four *FIG* genes, strongly suggest that the pheromone-induced expression of these genes in haploid cells of both mating types is because of direct regulation by Ste12p.

Table II. Induction of Gene Expression by  $\alpha$ -Factor

Gene	Fusion	Fold induction by pheromone
<i>FIG1</i>	P158A	36.9
<i>FIG2</i>	P294A	268.1
<i>KAR5/FIG3</i>	P900	67.9
<i>FIG4</i>	P403A-2	44.7
<i>TY</i> element	P105A-2	69.1
<i>FUS2</i>	P105A-1	798.9
<i>STE6</i>	P372B	6.2
<i>AFR1</i>	P313B	59.3
<i>CIK1</i>	P524B	19.4
<i>PCL2</i>	P342A	35.0
<i>RVS161</i>	P532C	6.5
<i>SPO11</i>	P436A-2	6.0
<i>ALK1</i>	P359A	70.2
<i>HOG1</i>	P423A	56.6
<i>PHD1</i>	P2B	7.0
<i>GAP1</i>	P534C	5.4
<i>AMD1</i>	P713	2.2
<i>YFL056c</i>	P104A	1.32
<i>YGR111w</i>	P9B	2.1
<i>YLR057w</i>	P430B	196.6
<i>YNR069c-YNR070w</i>	P482B	25.7
<i>YFL027c</i>	P28A	28.3
<i>YSC8010</i>	P452A	15.1
<i>CHRXV</i>	P439B	6.8
<i>YSCP9584.4</i>	P28B-2	1.93

**Four Novel Pheromone-induced Genes Are Important for Yeast Mating**

To begin the characterization of the pheromone-regulated genes identified from our screen, the mating phenotypes of 20 haploid mutant strains carrying different transposon insertions were analyzed (Table I). Haploid strains containing the *lacZ* insertions were derived from *MATa/MATa* diploid parental insertion strains and examined for defects in (a) viability; (b) cell cycle arrest and polarized growth in response to pheromone; (c) pheromone sensitivity and adaptation; (d) pheromone production in each cell type; and (e) mating efficiency in both unilateral and bilateral matings (i.e., a *lacZ* insertion strain  $\times$   $\alpha$  wild-type or a *lacZ* insertion strain  $\times$   $\alpha$  *lacZ* insertion strain, respectively). No defects in viability, cell cycle arrest, polarized projection formation, adaptation, or pheromone production were detected for the strains that were examined. Evaluation of mating efficiencies under conditions of reduced cell densities, however, did identify three mutant strains, *fig1::lacZ*, *fig2::lacZ*, and *fig3::lacZ* that were each altered in mating efficiency relative to a wild-type strain.

The roles of *FIG1*, *FIG2*, and *KAR5/FIG3* in yeast mat-

Table III. Induction of Gene Expression by Low Nitrogen Medium

Gene	Fusion	Low nitrogen induction
<i>GAP1</i>	P534C	276.8
<i>DUR1,2</i>	P809	35.7
<i>AMD1</i>	P713	27.8
<i>PHD1</i>	P33A	13.5
<i>YFL056c</i>	P104A	3.0

Gene	Site	Location
<i>FIG1</i>	TGAAACG	-405
	*TGAAACC	-217
	*TGACACA	-206
	TGAAACG	-173
<i>FIG2</i>	TGAAATA	-133
	*TGAAACA	-449
	*TGAAAAA	-413
	TAAAAACA	-365
<i>KAR5/FIG3</i>	<u>TGAAACA</u>	-354
	*TAAAAACA	-291
	*TGACACA	-140
	*TAAAAACA	-122
<i>FIG4</i>	*AGAAACA	-22
	TTAAACA	-88
	TGAAACG	-40
Consensus	AGAAACA	-9
	TGAAACA	

Figure 2. Sequences similar to the consensus Ste12p binding site in the upstream regions of the *FIG1*, *FIG2*, *KAR5/FIG3*, and *FIG4* genes. Sites preceded by an asterisk indicate they occur on the opposite strand. Underlined sequences represent exact matches to the PRE consensus sequence.

ing were investigated in detail using a variety of mating conditions. Because of its striking pheromone-induced expression pattern and its homology to the yeast Sac1p, a known effector of actin cytoskeletal dynamics (Cleves et al., 1989; Novick et al., 1989), the role of *FIG4* in mating was also examined. Although initial studies failed to reveal a mating defect in *fig4::lacZ* strains, it is possible that the transposon insertion allele that was tested, P403A-2, may encode a fusion protein that retains some level of Fig4p activity, as it contains 90% of the Sac1p homology domain (see below). To ensure that null phenotypes were analyzed, strains in which the entire protein coding sequence of each of these genes was substituted with *URA3* were constructed by PCR (Baudin et al., 1993). The *fig1Δ*, *fig2Δ*, *kar5Δ/fig3Δ*, and *fig4Δ* strains grew at rates identical to those of wild-type cells, and no vegetative growth defects were apparent at 16°, 25°, 30°, and 37°C.

As observed with the transposon insertion alleles, *fig1Δ*, *fig2Δ*, *kar5Δ/fig3Δ*, and *fig4Δ* mutants appeared normal for cell cycle arrest and recovery, pheromone sensitivity, and projection formation at all pheromone concentrations tested (Fig. 3 for mating projection results; refer to Materials and Methods). However, the *figΔ* strains each exhibited quantitative mating defects, and the severity of the defect differed depending upon the mating condition (Table IV). At 30°C, absence of Fig1p, Kar5/Fig3p, or Fig4p results in a bilateral mating defect that reduces mating efficiency 2.5-, 77.4-, and 2.9-fold, respectively, relative to that of a wild-type strain. In contrast, loss of Fig2p reproducibly increases the mating efficiency 3.2–7.2-fold in both unilateral and bilateral matings. Increased mating efficiency through the loss of a gene product in otherwise wild-type cells is a novel phenotype for a gene that functions in mating. The increased mating efficiency for *fig2Δ* strains is likely because of their enhanced agglutination relative to wild-type cells (see below). The mating phenotypes of the *fig1Δ*, *fig2Δ*, and *kar5Δ/fig3Δ* strains were the same as their respective transposon insertion mutants. We also tested the relative mating efficiencies of *fig1Δ*, *fig2Δ*, and *fig4Δ* mutants using mating conditions that concentrate cells on filters (Sprague, 1991). Under these conditions, the relative mating efficiencies of *fig1Δ* and *fig4Δ* were similar to those observed by liquid conditions. The increased mating efficiency of *fig2Δ* strains was no longer observed; instead we observed a 6.6-fold decrease in mat-

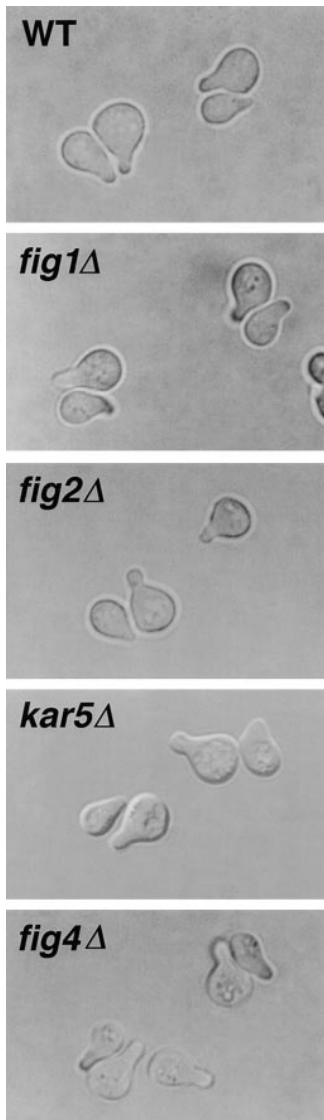


**Figure 3.** Mating projection formation by *MATa* wild-type and *figΔ* cells in the presence of isotropic mating pheromone. Cells shown were treated for 2 h with  $\alpha$ -factor mating pheromone at a concentration of 5  $\mu$ g/ml. *figΔ* cells treated with reduced concentrations of pheromone and/or examined at additional timepoints (i.e., 1, 4, 6 h after treatment) also appeared normal in the shape, number, and rate of appearance of mating projections relative to wild-type cells.

ing efficiency relative to wild-type strains. We presume that in contrast to liquid mating conditions that require cells to agglutinate to mate efficiently (Kurjan, 1993), the close packing of cells caused by collection on filters reduces or eliminates the need for agglutination in the filter-mating assays. As noted below, the increased mating efficiency of *fig2Δ* strains in liquid assays is likely due to the hyperagglutination activity of these cells; this activity is no longer expected to be important in filter-mating assays.

We also investigated the effects of different conditions on the mating efficiencies of *fig1Δ*, *fig2Δ*, and *fig4Δ* mutants (Table IV); the severe effect of the *kar5Δ/fig3Δ* mutation on mating efficiency precluded its accurate measurement under these conditions. At 16°C, the mating efficiencies of both *fig1Δ* and especially *fig2Δ* bilateral matings are impaired relative to wild-type strains (1.4- and 18-fold, respectively). The bilateral matings involving *fig1Δ* and *fig2Δ* mutants are also inhibited more strongly than wild type by polymyxin B sulfate, a membrane-disrupting agent. The effects of PEG and EGTA on the mutant matings revealed additional differences between the *fig1Δ* and *fig2Δ* strains. While PEG is a potent (5.2–7.6-

fold) enhancer of mating efficiency for wild-type, *fig1Δ*, and *fig4Δ* strains, it has a much smaller effect on the mating efficiency of *fig2Δ* strains. Interestingly, the mating efficiency of *fig1Δ* bilateral matings is more sensitive to EGTA, exhibiting a 3.1-fold decrease relative to wild-type strains. The relative mating efficiency of *fig4Δ* mutants was affected to similar degree as the mating efficiency of wild-type strains by the different conditions. In summary, the differing effects of the conditions of cold temperature, PEG, and EGTA on the mating efficiencies of *fig1Δ*, *fig2Δ*, and *fig4Δ* strains suggest that Fig1p, Fig2p, and Fig4p play distinct roles in mating, and may provide insights into their molecular functions (see Discussion).

### ***fig2Δ* and *kar5/fig3Δ* Mating Cells Hyperagglutinate and Form Small Colonies, Respectively**

After the discovery that *figΔ* mutants exhibit altered mating efficiencies, we sought to determine the phenotypic basis of these effects. Two macroscopic phenotypes were observed in matings involving *fig2Δ* and *kar5/fig3Δ* mutants. During mating, wild-type cells gather into clusters through agglutination. *fig2Δ* strains exhibit a hyperagglutination phenotype in which mating cells aggregate to a greater extent than wild-type cells. This phenotype is observed by both uni- and bilateral crosses using settling assays (Fig. 4 A), and microscopic examination of mating cells (data not shown). Hyperagglutination caused by the *fig2Δ* mutation is an interaction specific to mixtures of mating cells; *fig2Δ* mutant strains of either mating type do not aggregate during vegetative growth or when mixed with cells of the same mating type. Hyperagglutination of *fig2Δ* strains during mating was observed at both 30°C and 16°C, indicating that the cold sensitivity of *fig2Δ* mutant matings is caused by a defect independent of agglutination.

The second macroscopic mating phenotype occurs in bilateral crosses of *kar5/fig3Δ* mutants. Matings of wild-type and all other *figΔ* mutant strains gave rise to uniformly-sized diploid colonies after 1.5 d of incubation at 30°C. In contrast, matings of *kar5/fig3Δ* mutants produced many small, irregular colonies as shown in Fig. 4 B. The number of smaller colonies approximates that of the total number of colonies formed in matings involving wild-type cells. Cells from both large and small colonies were fixed and then stained with Hoechst to examine their nuclear contents. Budding cells, cells with mating projections, anucleate and multinucleate cells, and zygotes were observed in each case. Progeny from both classes of colonies mated with both *MATa* and *MATα* tester strains. These phenotypes are consistent with nuclear fusion failures in *kar5Δ/fig3Δ* prezygotes (see below). Such failures would be expected to lead to unstable heterokaryons, which, in turn, produce haploid progeny.

### ***fig1Δ*, *fig2Δ*, and *fig4Δ* Strains Exhibit Defects in Mating Cell Morphology**

The mating properties of the *figΔ* mutant strains were investigated further by examining the morphology and distribution of nuclei in cells and zygotes in wild-type and bilateral *figΔ* mating mixtures (Fig. 5). Cell shape and degree of polarization (unpolarized, small–medium polar-

Table IV. Relative Mating Efficiencies of Wild-type, *fig1Δ*, *fig2Δ*, *kar5Δ/fig3Δ* and *fig4Δ* Strains

Strains			Filter	PEG	α factor	EGTA		Polymyxin B	
	30°C	16°C	30°C	6.7%	33 μg/ml	7.5 mM	15 mM	5 μg/ml	10 μg/ml
WT × WT	1.0 ± 0.4	1.0	1.0	1.0	1.0	1.0	1.0	1.0	1.0
		(-7.5×)		(+7.6×)	(-29.0×)	(-2.0×)	(-3.6×)	(-7.7×)	(-29.6×)
<i>fig1Δ</i> × WT	-1.2 ± 0.0	-1.0	—	+0.7	-0.8	-1.0	-1.0	-0.7	-1.7
<i>fig1Δ</i> × <i>fig1Δ</i>	-2.5 ± 0.2	-1.4	-3.3	+1.1	-0.8	-1.8	-3.1	-3.4	≥3.4 <sup>‡</sup>
<i>fig2Δ</i> × WT	+7.2 ± 1.6	-4.7	—	+0.3	-0.8	-1.0	-0.8	-1.0	-0.6
<i>fig2Δ</i> × <i>fig2Δ</i>	+3.2 ± 1.2	-18.0	-6.6	0.2	-1.0	-1.5	-1.4	-5.3	-2.7
<i>kar5Δ/fig3Δ</i> × WT	-1.2 ± 0.2	—	—	—	—	—	—	—	—
<i>kar5Δ/fig3Δ</i> × <i>kar5Δ/fig3Δ</i>	-77.4 ± 15*	—	—	—	—	—	—	—	—
<i>fig4Δ</i> × WT	-1.4 ± 0.25	-1.0	—	+1.0	-1.4	-0.8	-0.6	-1.0	-0.8
<i>fig4Δ</i> × <i>fig4Δ</i>	-2.9 ± 1.2	-0.8	-2.5	+1.7	-1.2	-0.6	-1.0	-0.7	-0.4

For each mating condition, the fold difference relative to wild-type matings (1.0) is presented. For wild strains, the values in parentheses are the differences in mating efficiency relative to 30°C. The relative mating efficiency at 34.5°C is similar to the results reported for 30°C.

\*The mating efficiency is estimated based on the number of large colonies. The mating defect is probably larger than this; see text.

<sup>‡</sup>This is a minimum estimate; no diploids were observed on one of the plates.

ized, and large polarized cells and zygotes) were quantified (Table V). Three of the *figΔ* mutations, *fig1Δ*, *fig2Δ*, and *fig4Δ*, each alter the morphologies of mating projections and zygotes in distinct ways.

*fig1Δ*, and to a lesser extent *fig4Δ*, mating mixtures have fewer medium and large polarized cells than wild-type or *fig3Δ* matings (Fig. 5; Table V). Many of the *fig1Δ* and *fig4Δ* cells that are polarized possess mating projections with tips that are broader and less focused than those of wild-type cells; for these strains the percentage of large cells with pointed projections was less than half that of wild-type cells or other *figΔ* mutants (Fig. 5, insets; Table V). In addition, in the case of *fig4Δ* cells, we often observe multiple bumps around the cell periphery of unpolarized but enlarged cells, suggestive of failures in the initial establishment of mating cell polarity. We also examined the distribution of actin in these strains by rhodamine conjugated-phalloidin staining (Fig. 6). The pattern of actin staining at the mating projection tip is typically less intense and more dispersed in both *fig1Δ* and *fig4Δ* cells compared to that of wild-type cells, whereas actin polarization remains normal in *fig2Δ* cells. Thus, whereas *FIG1* and *FIG4* are dispensible for forming normal projections in isotropic levels of mating pheromone, in mating mixtures these genes are important both for the execution of cell polarization and the development of mating projection shape (see Discussion). Although the effects of the *fig1Δ* and *fig4Δ* mutations on cell polarization are similar, differences in zygote morphologies between these two mutants suggest they perform different functions in the mating process; *fig1Δ*, but not *fig4Δ*, zygotes display cell fusion defects (Fig. 5, and see below).

The morphological alterations in mating projection formation caused by the *fig2Δ* mutation are distinct from those generated by the *fig1Δ* and *fig4Δ* mutations. *fig2Δ* cells form hyperpolarized mating projections that are often narrower and longer than those of wild-type cells (Fig. 5). A consequence of the hyperpolarization of the *fig2Δ* mating projection is the formation of zygotes possessing narrow fusion bridges (the central portion of zygotes formed by fusion between the polarized tips of mating cells) (Fig. 5). Measurement of the ratio of fusion bridge width/average parental cell pair width for 50 wild-type,

*fig1Δ*, and *fig2Δ* zygotes supports this observation; for wild-type and *fig1Δ* zygotes these ratios are 0.52 and 0.51, respectively, whereas for *fig2Δ* zygotes the value is 0.30. Thus, *FIG2* is important for mating cell projection shape and conjugation bridge diameter.

While preparing this manuscript, we learned that *FIG3* corresponds to the previously identified *KAR5* gene, whose molecular characterization has not been reported. Analysis of cell polarization and zygote formation in *fig3Δ* mutant cells indicated that cell polarization and zygote morphology is normal, unlike that of *fig1Δ*, *fig2Δ*, and *fig4Δ* mating cells. Instead, *kar5Δ/fig3Δ* zygotes displayed nuclear fusion defects in which nuclei lie within close proximity but fail to fuse (Fig. 5). This result is consistent with that reported previously for *kar5* mutant alleles (Kurihara et al., 1994; Fig. 5, this study).

### *FIG1* and *FIG2* Function in Cell Fusion and Nuclear Migration

To help understand the functions of *FIG1* and *FIG2* in the differentiation of wild-type mating cells, we examined the cell morphologies and nuclear positions of prezygotes and zygotes formed by wild-type, *fig1Δ*, and *fig2Δ* strains mated at 16°C; this condition enhances the mating defects of the mutant strains. As observed for *fig1Δ* strains at 30°C, *fig1Δ* and *fig2Δ* zygotes formed at 16°C display cell fusion defects. These defects were quantified by examining prezygotes and zygotes using DIC microscopy, DAPI staining (to examine nuclear fusion and morphology), and staining with the lipophilic dye FM4-64 which decorates lipids and membranes, but not cell wall material (Fig. 7). As shown in Table VI, the incidence of partial and complete failures in cell fusion is increased markedly in *fig1Δ* zygotes (ninefold), and more modestly in *fig2Δ* zygotes (approximately twofold).

When *fig2Δ* strains mate at both 30° and 16°C, a high frequency (84%) of zygotes show the hyperpolarization/narrow fusion bridge phenotype. As shown in Fig. 7, a number of defects appear to be caused by the narrow fusion bridge phenotype of *fig2Δ* mutants. The most prevalent phenotype, observed in ~80% of *fig2Δ* zygotes, is a novel nuclear morphology that suggests a failure to com-

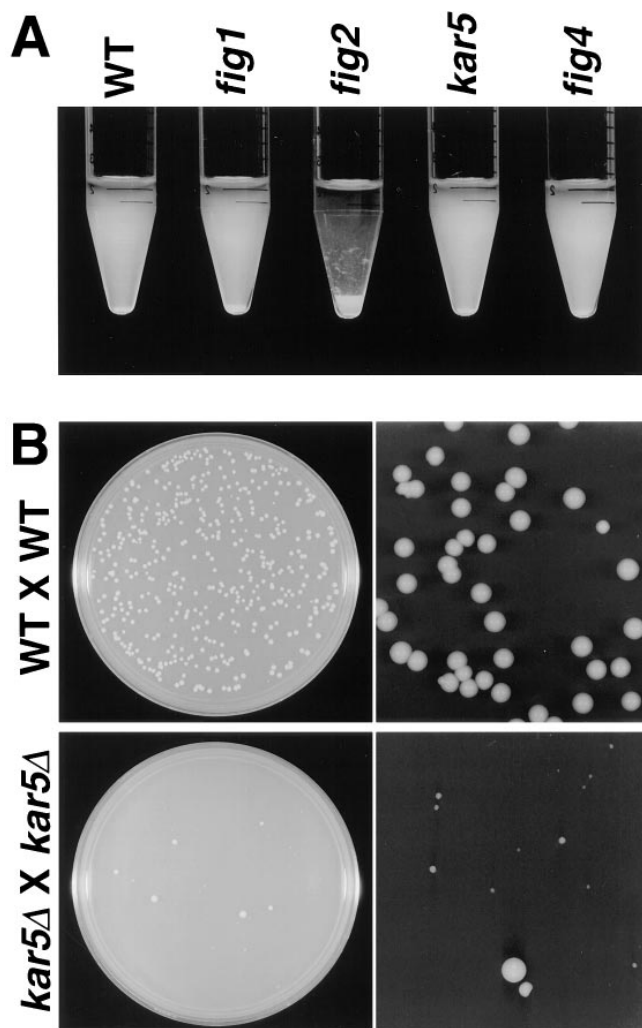


**Figure 4.** Hyperagglutination and small colony phenotypes observed in matings of *fig2Δ* and *kar5Δ/fig3Δ* strains. (A) Unilateral and bilateral matings involving *fig2Δ* strains cause hyperagglutination, observable as rapid sedimentation of extensive cell clusters. Depicted are bilateral matings of wild-type and *figΔ* strains. (B) Bilateral matings of *MAT $\alpha$  kar5Δ/fig3Δ* and *MAT $\alpha$  kar5Δ/fig3Δ* cells often produce very small colonies. The left panels are magnifications of sections of the plates shown on the right. Plates were incubated for 36 h. The large colonies are visible after 1 d. Both large and small colonies from the *kar5Δ/fig3Δ* matings contain abnormal cells as described in the text.

ple the late steps of nuclear fusion. Normally, nuclear fusion proceeds by the microtubule-dependent congression of nuclei, followed by nuclear membrane fusion (Kurihara et al., 1994). The fused haploid nuclei then form a contiguous, elliptical or quasispherical diploid nucleus. In wild-type zygotes possessing a bud, the nucleus is often located near the site of bud emergence, or can be seen to be segregating or to have segregated between the zygote and bud (Fig. 7; top two rows). In *fig2Δ* zygotes, the newly fused nucleus nearly always has an abnormal shape, and in zygotes possessing a bud it is frequently observed to lie in abnormal positions, suggesting difficulties in nuclear migration to the bud site or in subsequent segregation events (Fig. 5; Fig. 7, bottom two rows; Table VI). *fig2Δ* zygotes appear delayed in rounding up of the nucleus, as judged by

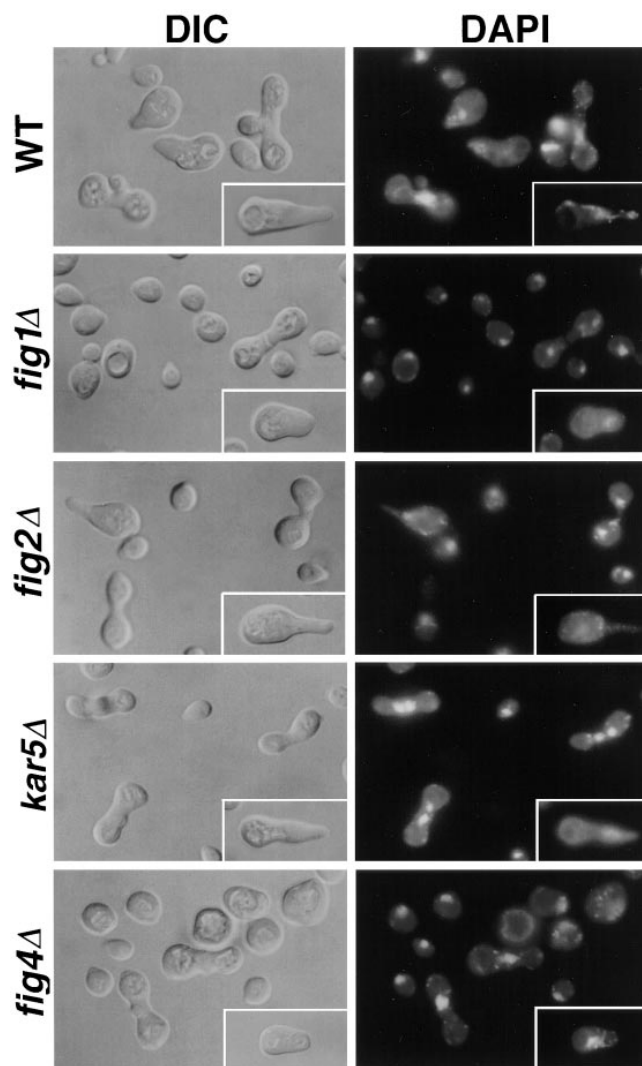


**Figure 5.** Mating mixtures of wild-type and *figΔ* cells reveal cell polarization and zygote formation defects. Bilateral matings are shown. The inset shows a typical polarized mating cell. Note the *fig1Δ* prezygote has a septum indicative of a failure in cell fusion. *fig2Δ* zygotes have a narrow bridge. *kar5Δ* zygotes have two unfused nuclei in close proximity.

the presence of contiguous DAPI staining material across the fusion bridge region (Fig. 7, Table VI). In the majority of these nuclear configurations, two interconnected DAPI staining regions are observed on either side of the fusion bridge, whereas less frequently a single DAPI staining region is observed to be contiguous with nuclear material remaining in the fusion bridge (Table VI). For each of these cases, the majority of these altered nuclear configurations occur in *fig2Δ* zygotes displaying the narrow bridge phenotype shown in Figs. 5 and 7.

To further examine the cell and nuclear fusion defects visualized by light microscopy, we performed electron microscopic analysis on thin section preparations of wild-type, *fig1Δ*, and *fig2Δ* zygotes (Fig. 8). Inspection of micrographs of the *fig1Δ* zygotes confirms the presence of undissolved cell wall materials and membrane causing both partial and complete fusion defects (Fig. 8, B and C; this is particularly evident in higher magnification micrographs; data not

Table V. Morphologies of Cells in Wild-type and *figΔ* Mutant Mating Mixtures

	Zygotes	Unpolarized	Small-medium polarized	Large polarized	Pointed projections
Wild-type	9.0	44.1	42.4	3.1	64.2
<i>fig1Δ</i>	5.0	69.3	24.5	1.1	29.5
<i>fig2Δ</i>	2.9	55.3	40.0	2.0	70.1
<i>fig3Δ</i>	4.8	50.7	40.8	3.7	59.1
<i>fig4Δ</i>	6.1	54.2	36.5	3.1	24.1

At least 500 cells were scored to determine the percentage of each class of cells. Quantitation of the percentage of pointed projection tips of large polarized cells was based on observations of  $\geq 250$  cells.

shown). Moreover, examination of the partial fusion defects by both fluorescent microscopic techniques and electron microscopy indicates that nuclear fusion is a robust process, capable of being executed through very small regions of cytoplasmic continuity (for example, Fig. 7, *fig1Δ* center panel; Fig. 8 C; and Table VI, partial fusion defect column). Analysis of *fig2Δ* zygotes revealed elongated nuclear morphologies consistent with those visualized by DAPI staining of whole zygotes. In summary, these different data demonstrate that *fig1Δ* and *fig2Δ* zygotes exhibit both cell fusion and nuclear morphology defects.

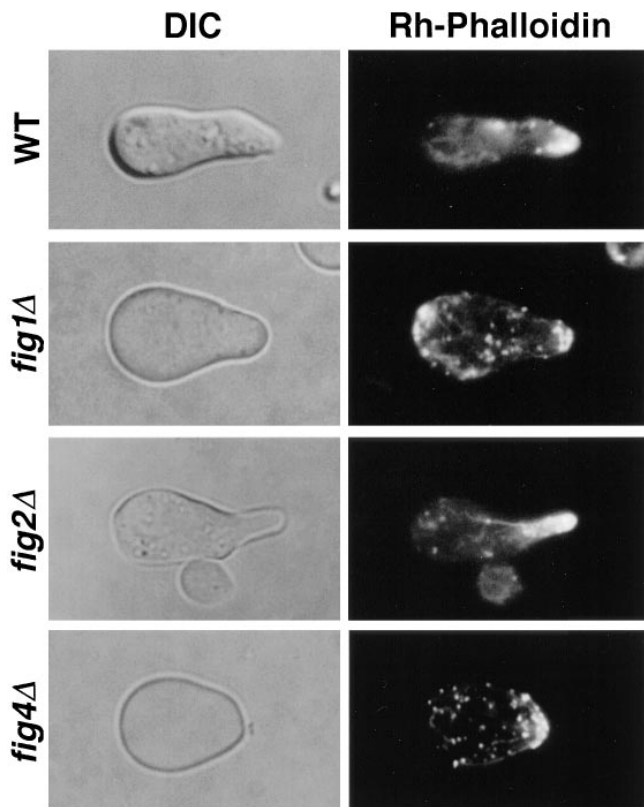


Figure 6. Actin distribution in wild-type, *fig1Δ*, *fig2Δ* and *fig4Δ* polarized cells containing mating projections. Cells shown are derived from mating mixtures stained with rhodamine-conjugated phalloidin after fixation. *fig1Δ* and *fig4Δ* cells typically contain less actin at the growing tip of the mating projection, whereas actin distribution in *fig2Δ* appears similar to that of wild-type cells.

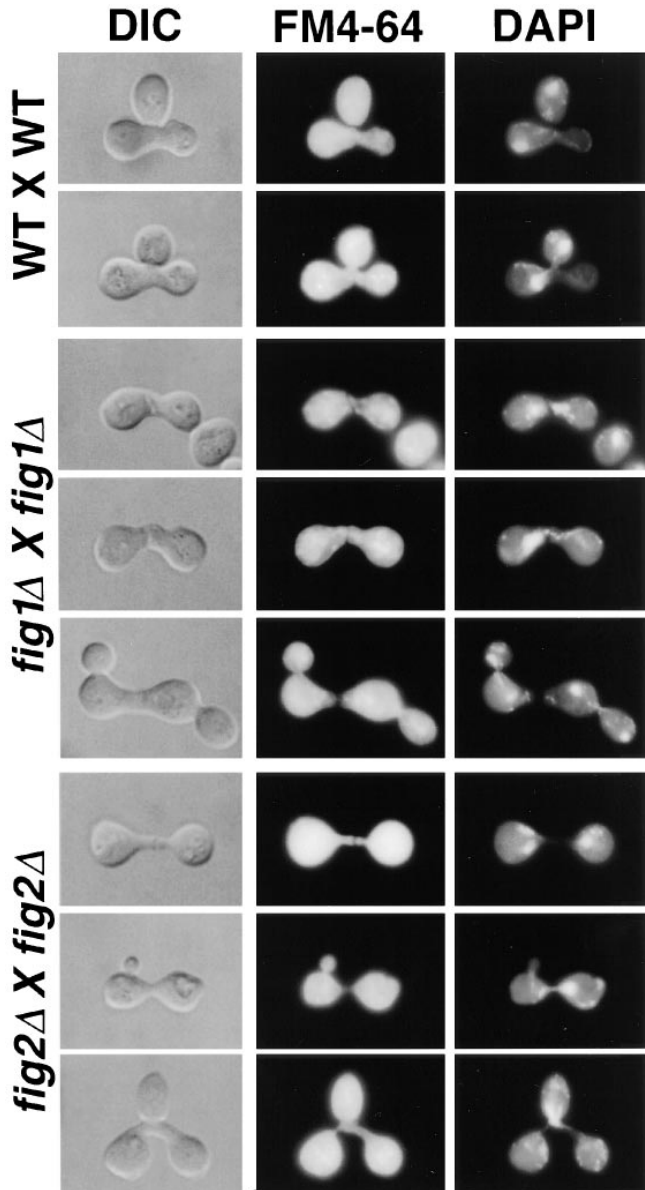


Figure 7. Cell fusion and nuclear morphology defects in *fig1Δ* and *fig2Δ* zygotes incubated at 16°C. Left panels are zygotes as viewed by DIC. Center panels show the same zygotes stained with the lipophilic dye *FM4-64*; the dye stains lipids and membrane, but not cell wall material. Panels at right show *DAPI* staining of nucleic acids within zygotes. *fig1Δ* zygotes often display complete (top and bottom rows) or partial (middle row) fusion defects. *fig2Δ* zygotes have narrow conjugation bridges, and often have cell fusion defects (top two rows) or nuclear migration/segregation defects (bottom two rows).

#### *FIG1*, *FIG2*, and *FIG4* Function in at Least Two Different Mating Cell Differentiation Pathways Required for Cell Shape and Polarity

The different effects of nonoptimal mating conditions on the mating efficiencies of *fig1Δ*, *fig2Δ*, and *fig4Δ* strains suggested that these mutants are defective in different pathways involved in mating cell differentiation (Table IV). To investigate this further, we examined the epistatic relationships of the *figΔ* mutations by characterizing the mat-

Table VI. Cell Fusion and Nuclear Morphology Defects in Wild-type, *fig1Δ* and *fig2Δ* Zygotes

30°							N
WT × WT	95	0.5	2.5	0.5	0	1.5	200
<i>fig1Δ</i> × <i>fig1Δ</i>	77	0.4	14	9	0	0	231
<i>fig2Δ</i> × <i>fig2Δ</i>	15	0.5	3.3	2.9	59	20	208
16°							N
WT × WT	95	0.9	1.4	2.3	0	0	217
<i>fig1Δ</i> × <i>fig1Δ</i>	45	0.5	33	21	0	0	204
<i>fig2Δ</i> × <i>fig2Δ</i>	8	2	3.9	4	52	30	212

Values represent percentages of the total number of zygotes examined (N).

ing cell projection and zygote morphologies of double mutant strains mated at 30° and 16°C; bilateral matings of *MATa* and *MATα* *fig1Δfig2Δ*, *fig1Δfig4Δ*, and *fig2Δfig4Δ* mutant strains were examined (Fig. 9). For most of the double mutant strains, the phenotype of any single mutation was never completely epistatic to that of another (Table VII). All double mutants carrying the *fig1Δ* mutation displayed reductions in the fraction of cells producing pointed mating projections and increases in the rate of cell fusion defects. Similarly, double mutants involving the *fig2Δ* mutation displayed a narrow conjugation bridge and the aberrant nuclear morphology phenotypes; these mutants also hyperagglutinated at both 30° and 16°C. All double mutants involving the *fig4Δ* mutation displayed a reduction in the percentage of cells with pointed projections. Thus, the morphological phenotypes of the *fig1Δfig2Δ* and *fig2Δfig4Δ* double mutants represent a combination of those observed in each of the corresponding single mutants, suggesting that Fig2p functions in a distinct pathway from that of either Fig1p or Fig4p (Table VII).

There are exceptions to these independent epistasis relationships. The *fig1Δ* and *fig4Δ* mutations did not produce additive effects in cell polarization, suggesting that these mutants may function in the same or significantly overlapping pathways for this particular process (Table VII; however, see Discussion). In addition, the fraction of cells with a pointed projection tip in the *fig1Δfig2Δ* and *fig2Δfig4Δ* mutants was reduced relative to that of *fig2Δ* mutants alone (Table VII). This suggests that hyperpolarization caused by the absence of Fig2p function may partly require the function of the polarization pathway(s) in

which Fig1p and Fig4p function. We are cautious, however, in interpreting this relationship as one that applies to normal mating cell polarization, since hyperpolarization is a consequence of the loss of *FIG2* function and not a polarization event normally occurring in wild-type mating cells. In summary, these results indicate that the *FIG1*, *FIG2*, and *FIG4* genes encode proteins that are components of at least two distinct mating cell differentiation pathways required for projection shape and polarity.

### Fig1p and Fig2p Localize to the Cell Periphery

To gain further insight into the function of the different pheromone-regulated genes, the subcellular localizations of β-gal fusion proteins in 14 strains carrying *lacZ* fusions to different genes, including *fig1::lacZ*, *fig2::lacZ*, *fig3::lacZ*, and *fig4::lacZ*, were analyzed using anti-β-gal antibodies and indirect immunofluorescence. Fusion proteins encoded by *fig3::lacZ* and *fig4::lacZ*, along with those from 10 other strains, failed to localize in a discrete pattern or at a level above background. Presumably, some of these fusion proteins may lack sequences required for their stability or subcellular localization. Two strains, *fig1::lacZ* and *fig2::lacZ*, were, however, found to exhibit strong β-gal staining at discrete sites in pheromone-treated cells (Fig. 10). In each case the β-gal fusion proteins appeared to be abundant, based on staining intensity, and localized to the cell periphery in 100% of the cells ( $n > 400$ ). The Fig1::β-gal and Fig2::β-gal fusion proteins were often slightly polarized toward the projection tips, but did not appear to be as sharply concentrated at the tips as reported previously for the Fus1 and Fus2 proteins (Trueheart et al., 1987; Elion et al., 1995). For both Fig1::β-gal and Fig2::β-gal fusions (~10%), in a small fraction of cells perinuclear staining was observed (Fig. 10). Such staining was also observed in rare cells (<3%) that were not treated with pheromone and the staining was very weak (Fig. 10). This perinuclear staining may represent low levels of the fusion proteins contained in the endoplasmic reticulum. The localization of Fig1p and Fig2p suggests they may perform their functions at the cell periphery.

### The *FIG1*, *FIG2*, *KAR5/FIG3*, and *FIG4* Proteins Contain Distinct Sequence Features

The four genes characterized in detail in this study, *FIG1*,

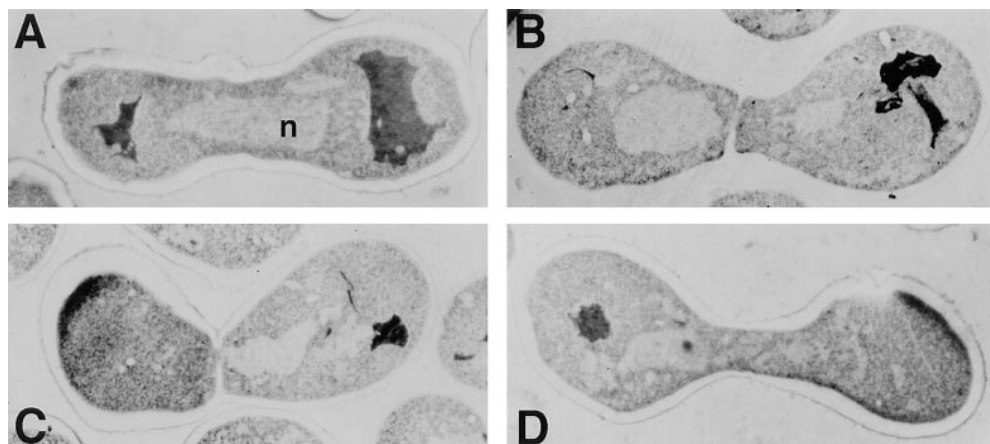


Figure 8. Electron micrographs of thin sections through zygotes formed from bilateral matings. (A) wild-type; (B) *fig1Δ* mutant, complete fusion defect; (C) *fig1Δ* mutant, partial fusion defect; and (D) *fig2Δ* mutant, note narrow fusion bridge. *n* indicates the nucleus.

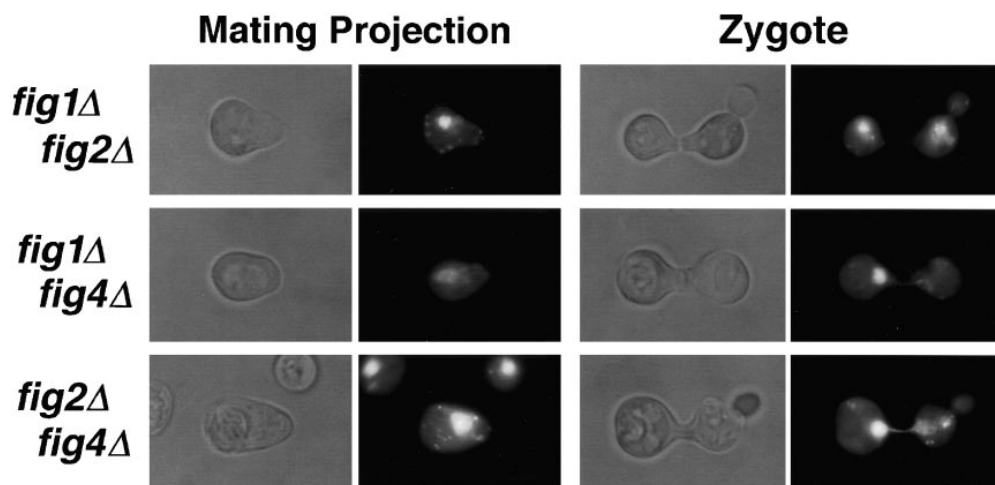


Figure 9. Phenotypes of double *figΔ* mutants affecting mating projection and zygote morphology. A typical polarized cell (Mating Projection) and zygote from bilateral matings of *fig1Δ fig2Δ* cells (top), *fig1Δ fig4Δ* cells (middle) and *fig2Δ fig4Δ* cells (bottom) is shown.

*FIG2*, *KAR5/FIG3*, and *FIG4*, are predicted to encode proteins of 298-, 1609-, 504-, and 879-amino acids, respectively. Each of these proteins is predicted to contain domains suggestive of a structure, localization, or function of the proteins. (Fig. 11 A).

*FIG1* and *FIG2* are predicted to encode membrane-associated proteins. Fig1p contains four predicted transmembrane (TM) domains with a loop between the first and second TM segments that is expected to be extracellular and contain several potentially glycosylated residues (Fig. 11 A). The protein has several features in common with members of the four transmembrane (4TM) superfamily of proteins (Wright and Tomlinson, 1994), including the transmembrane segments, the potential extracellular glycosylated loop, and the location of polar and charged residues at conserved points within two of the TM domains (N23 in TMD1 and D255 in TMD4) (Wright and Tomlinson, 1994). Fig2p contains a predicted signal peptide at its amino terminus and potential glycosyl phosphatidylinositol (GPI) anchor sequence at its carboxy terminus. The protein is serine/threonine rich (44.5% serine or threonine) as are many extracellular proteins, and contains many potential *N*-linked glycosylation sites (Klis, 1994; Cid et al., 1995).

Table VII. Morphologies of Cells in Wild-Type and *figΔ* Double-Mutant Mating Mixtures

	Pointed projections		Cell fusion defects		Narrow bridge	
	30°C	30°C	16°C	30°C	16°C	
Wild-type	64	2	3	1	1	
<i>fig1Δ</i>	20	15	66	2	0	
<i>fig2Δ</i>	65	15	11	98	100	
<i>fig4Δ</i>	20	2	4	1	5	
<i>fig1Δ fig2Δ</i>	45	56	48	84	99	
<i>fig1Δ fig4Δ</i>	16	13	13	0	4	
<i>fig2Δ fig4Δ</i>	29	22	22	32	91	

At least 50 zygotes were scored to determine the percentage of zygotes possessing cell fusion defects and/or a narrow conjugation bridge morphology. Quantitation of the percentage of polarized cells with pointed projection tips was based on observations of  $\geq 100$  cells.

The sequence of *KAR5/FIG3* is predicted to encode a protein capable of containing several long coiled-coil domains (i.e.,  $\alpha$  helical regions with heptad repeats of hydrophobic residues) in the center of the protein. A protein of

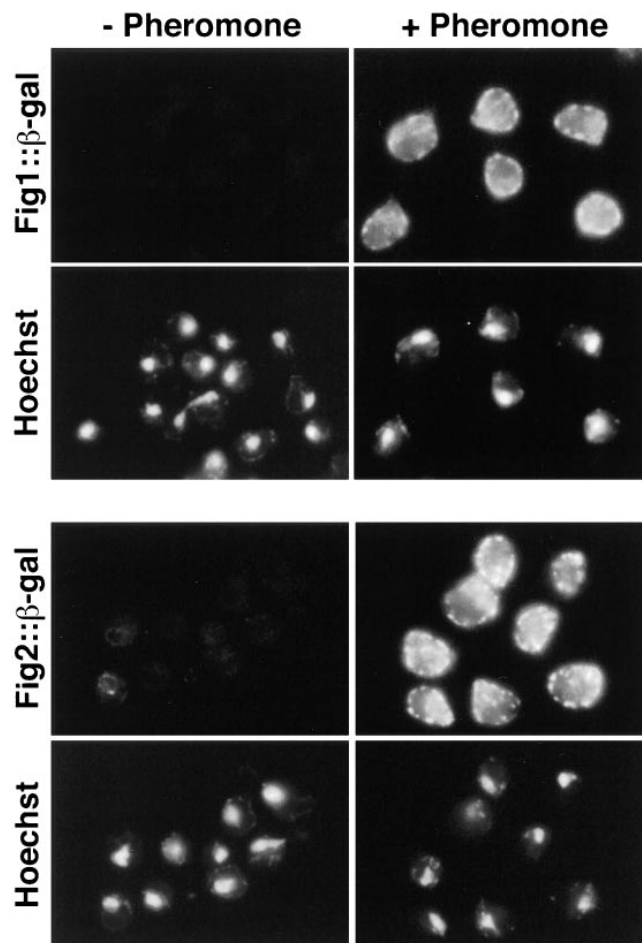


Figure 10. Localization of Fig1:: $\beta$ -gal and Fig2:: $\beta$ -gal fusion proteins. Cells were incubated in the absence or presence of mating pheromone for 2 h and then stained with anti- $\beta$ ::gal antibodies by indirect immunofluorescence. Staining was not detected in control strains that lacked  $\beta$ -gal fusions (data not shown). Hoechst 33258 was used to visualize DNA in the cells (bottom rows).



Table VIII. Strain List

Strain	Genotype
Y800	<i>MATa cry<sup>r</sup>/MATα CRY ura3-52/ura3-52 leu2-Δ98/leu2-Δ98 HIS3/his3-Δ200 TRP1/trp1-Δ1</i>
Y1400	<i>MATa cry<sup>r</sup> ura3-52 leu2-Δ98 his3-Δ200 trp1-Δ1</i>
Y1401	<i>MATα CRY ura3-52 leu2-Δ98 his3-Δ200 TRP1</i>
Y1402	<i>MATa cry<sup>r</sup> ura3-52 leu2-Δ98/leu2-Δ98 his3-Δ200 trp1-Δ1 bar1::HIS3</i>
Y1405	<i>MATa cry<sup>r</sup>/MATα CRY ura3-52/ura3-52 leu2-Δ98/leu2-Δ98 his3-Δ200/his3-Δ200 TRP1/trp1-Δ1 bar1::HIS3/bar1::HIS3</i>
Y1406	<i>MATa cry<sup>r</sup>/MATα cry<sup>r</sup> ura3-52/ura3-52 leu2-Δ98/leu2-Δ98 his3-Δ200/his3-Δ200 TRP1/trp1-Δ1 bar1::HIS3/bar1::HIS3</i>
Y1411	<i>MATa cry<sup>r</sup> ura3-52 leu2-Δ98 his3-Δ200 trp1-Δ1 bar1::HIS3</i>
Y1407	<i>MATa ura3-52 his3-Δ200 TRP1</i>
Y1408	<i>MATα ura3-52 HIS3 trp1-Δ1</i>
Y1409	<i>MATa his3-Δ200 TRP1 fig1::URA3</i>
Y1410	<i>MATα ura3-52 HIS3 trp1-Δ1 fig1::URA3</i>
Y1411	<i>MATa ura3-52 his3-Δ200 TRP1 fig2::URA3</i>
Y1412	<i>MATα ura3-52 HIS3 trp1-Δ1 fig2::URA3</i>
Y1421	<i>MATa ura3-52 his3-Δ200 TRP1 kar5/fig3::URA3</i>
Y1422	<i>MATα ura3-52 HIS3 trp1-Δ1 kar5/fig3::URA3</i>
Y1433	<i>MATa ura3-52 his3-Δ200 TRP1 fig4::URA3</i>
Y1434	<i>MATα ura3-52 HIS3 trp1-Δ1 fig4::URA3</i>
Y1450	<i>MATa sst2</i>
Y1451	<i>MATα sst2</i>

All strains from the Snyder laboratory collection.

pheromone-induced genes, a set of previously characterized genes was also found to be under pheromone regulation. The most frequently identified pheromone-regulated gene of this class was *SPO11*. *SPO11* is induced in meiosis, and Spo11p is found covalently attached to the ends of meiotic double-strand breaks in genomic DNA (Atcheson et al., 1987; Keeney et al., 1997). Our data suggests that *SPO11* is expressed in haploids and exhibits enhanced expression upon pheromone treatment. Consistent with pheromone regulation is the presence of two consensus PRE sites upstream of the *SPO11* coding sequence. *SPO11* does not promote recombination during mating, as matings of *MATa spo11Δhis4-280* cells to *MATα spo11Δhis4-260* cells did not reveal any change in the number of His<sup>+</sup> prototrophs relative to control matings with wild-type cells (data not shown). Spo11p, which localizes to the nucleus (Burns et al., 1994), might play a role in the organization of the diploid nucleus after nuclear fusion. This organization may occur soon after nuclear fusion as homologous chromosomes appear associated during vegetative growth (Weiner and Kleckner, 1994).

Several other pheromone-regulated genes that may function in mating were also identified by our screen. Two genes encoding proteins that might function in the cell cycle regulatory events that mediate pheromone-induced arrest and recovery are *HOG1* and *CKI3/YCK3*. A recent study has found that the *HOG1* osmoregulatory MAP-kinase pathway negatively regulates the activity of the mating pathway, based in part on the finding that pheromone sensitivity was greater in a *hog1Δ* strain than in a wild-type strain (Hall et al., 1996). *CKI3/YCK3* encodes one of the four casein kinase I homologous proteins found in *S. cerevisiae* (Robinson et al., 1992; Wang et al., 1996). *CKI3/YCK3* has recently been identified as a high copy suppressor of *gcs1* mutants that fail to reenter the cell cycle from stationary phase (Wang et al., 1996). Thus, *CKI3/YCK3* en-

codes a pheromone-induced protein that has activity as a cell cycle regulator.

Our study also found the cell polarity gene *RVS161* to be pheromone regulated. Rvs161p has recently been shown to be important for proper cell fusion and mating under certain conditions (Dorer et al., 1997). Mutations in the *RVS161* gene affect actin-dependent processes including diploid bud site selection and endocytosis (the gene is allelic to *END6*), and a mammalian homologue of Rvs161p, amphiphysin, has been predicted to be involved in synaptic vesicle recycling (Crouzet et al., 1991; David et al., 1994; Munn et al., 1995; McPherson et al., 1996). Perhaps Rvs161p acts to maintain the proper positioning and/or organization of the actin cytoskeleton to directly or indirectly control the local regulation of cell surface membranes and receptors. A possible role for Rvs161p in the regulation of pheromone receptors is particularly interesting in light of the common requirement for the function of these proteins in the process of cell fusion (see below; Brizzio et al., 1996; Elia and Marsh, 1996; Dorer et al., 1997).

Another interesting group of genes that we found to be regulated by mating pheromone are the pheromone-repressed genes. The novel gene *QORI*, as well as *FOX2* and *PHO81*, have been suggested or demonstrated to be subject to glucose repression (Minehart, S., S. Erdman, and M. Snyder, unpublished data; Johnston and Carlson, 1992; Kunau and Hartig, 1992; Timblin et al., 1996). The common property of glucose regulation suggests that the decreased expression levels of these genes in cells exposed to pheromone may occur through a common mechanism. Activation of the pheromone pathway may curb the expression of these genes directly by affecting a common regulator, as would be the case if glucose repression is established and/or maintained at the G1 phase of the cell cycle. Arrest of the cell cycle in G1 by pheromone would, in turn, reduce expression of these genes. Alternatively, repression by the pheromone pathway might work indirectly by altering the expression of upstream genes that participate in the sensing of nutrient levels, which then regulate the expression of the pheromone-repressed genes (Johnston and Carlson, 1992).

### *Some Pheromone-induced Genes Such as PHD1 Are Induced by Both Mating and Pseudohyphal Differentiation Signals*

We found that several genes are induced by both pheromone and pseudohyphal growth-promoting conditions (Tables I–III), suggesting that a common set of target genes may be involved in both processes. One of these genes is *PHD1*, whose overexpression enhances pseudohyphal growth in yeast, and whose product is a transcription factor capable of activating the expression of at least five potential target genes (Gimeno, 1994; Gimeno and Fink, 1994). A potential *PHD1* target, *CDC91*, was found in our screen, and a second target corresponds to the *DAL81* gene, which, like several of the genes identified in our screen (i.e., *GAPI*, *DURI2*, *AMD1*, and *YGR111w*), is involved in nitrogen metabolism (Magasanik, 1992). Thus, induction of Phd1p by low nitrogen conditions or pheromone may, in turn, activate a common set of target genes important for the processes of pseudohyphal growth and mating under certain conditions (see below).

The reason why induction of genes involved in nitrogen metabolism might be advantageous for mating is unclear. Perhaps the induction of these genes is a fortuitous vestige of their common activation mechanism. Previous studies have shown that several components of the Ste20p MAP-kinase signaling pathway (Ste20p, Ste11p, Ste7p) and the transcription factor, Ste12p, are used by both the mating and pseudohyphal pathways (Liu et al., 1993; Roberts and Fink, 1994). Nonetheless, the common induction of several genes by both pathways suggests they may share some common features and mechanisms. Consistent with this hypothesis, we have recently found that yeast cells exposed to low levels of mating pheromone form filamentous arrays similar to pseudohyphal cells (Erdman, S., and M. Malczynski, unpublished results). Similarly, the pheromone induction of genes that permit the use of alternative nitrogen sources may enable mating cells to grow through different environments in search of mates.

Although our work suggests a specific group of target genes shared by the pseudohyphal and pheromone-responsive pathways, others are unique to either of the two pathways. A previous study has shown that *FUS1* is not activated in cells undergoing haploid invasive growth and *FUS2*, *AFRI*, *ADP1*, *FIG1*, *FIG2*, and *KAR5/FIG3* are only induced by mating pheromone (Erdman, S., unpublished data; Roberts and Fink, 1994). Furthermore, a recent study has identified a gene, *TEC1*, whose product, along with Ste12p, appears to mediate the transcriptional induction of genes specific to pseudohyphal differentiation (Madhani and Fink, 1997). Thus, there remain many genes that are induced only during pseudohyphal growth or mating, presumably contributing to the unique aspects of these processes.

#### ***FIG1*, *FIG2*, *KAR5/FIG3*, and *FIG4* Identify New Components and Steps of the Yeast Mating Pathway**

Four novel pheromone-regulated genes characterized in this study play distinct roles in yeast mating. Strains in which the *FIG* genes are deleted display vegetative growth properties identical to those of wild-type strains, consistent with their specific involvement in the mating process. Analyses of the cell polarization behavior in mating mixtures of mutants revealed that Fig1p, Fig2p, and Fig4p are each necessary for normal mating projection formation; Kar5p/Fig3p is important for nuclear fusion.

Thus far, two major classes of proteins have been shown to be required for normal mating cell polarization: (a) general polarity components common to both budding and mating processes; and (b) pheromone-regulated components such as the pheromone receptor (Ste2p), Far1p, and Afr1p (Konopka et al., 1988; Konopka, 1993; Herskowitz et al., 1995; Konopka et al., 1995; Pringle et al., 1995; Roemer et al., 1996). Fig1p, Fig2p, and Fig4p, like the latter group of proteins, are induced by mating pheromone and appear to function in the specification and/or organization of pheromone receptor-dictated sites of polarized growth. However, a significant difference exists between the phenotypes of mutants in the *FIG1*, *FIG2*, and *FIG4* genes and those in *STE2*, *FAR1*, and *AFRI*. The *fig* mutants arrest and polarize normally in the presence of uniform concentrations of mating pheromone, but exhibit polarization

defects only in mating mixtures; *ste2*, *far1*, and *afr1* mutants exhibit defects under both conditions (Konopka et al., 1988; Chang and Herskowitz, 1990; Konopka, 1993; Chen-evert et al., 1994; Dorer et al., 1995; Konopka et al., 1995; Valtz et al., 1995). One principal difference between these two conditions is that in the presence of isotropic concentrations of pheromone, cells use axial and distal bud site polarity landmarks to specify sites of mating projection formation, whereas in mating mixtures cells choose projection sites on the basis of the pheromone receptors detecting gradients of mating pheromones that emanate from potential mating partners (Jackson and Hartwell, 1990; Madden and Snyder, 1992; Segall, 1993; Valtz et al., 1995). These different conditions also produce distinct cell morphologies and may reveal differing aspects of the mating process (Figs. 3 and 5; Madden and Snyder, 1992; Rose and Marsh, 1997). Interestingly, strains lacking either *FIG1* or *FIG2* also possess cell fusion defects; the cell fusion process has also been speculated to be regulated by cell-cell contact (Rose and Marsh, 1997). Thus, from the specific requirements for *FIG1*, *FIG2*, and *FIG4* for normal mating cell projection polarization and shape in mating mixtures, we conclude that the products of these genes perform cell polarity functions associated with polarized growth sites that are dictated by cell-cell communication events.

The mating projection defects of the *fig* mutants provide three important insights into the process of mating projection formation. First, a number of proteins in distinct pathways participate in cell polarity events governing mating projection growth. Differences observed in the sensitivities of *fig1Δ*, *fig2Δ*, and *fig4Δ* mutants in the genes to specific mating conditions suggests that the *Fig1*, *Fig2*, and *Fig4* genes function primarily in distinct pathways. Phenotypic analyses of the mating cell polarization and cell fusion properties of double mutants clearly indicate that *FIG2* functions in a different pathway from that of *FIG1* and *FIG4*. Genetic arguments suggest that *FIG1* and *FIG4* function in the same or extensively overlapping pathways based on their lack of additive effects on projection tip shape. However, mutants in these genes display a number of distinct properties (e.g., EGTA sensitivity and cell fusion defects in *fig1Δ* mating cells), suggesting they may contribute to cell polarization in different ways. The epistatic relationship of the *FIG1* and *FIG4* genes will be ascertained more precisely after additional molecular characterization of the functions of these genes.

Second, although a number of gene products participate in cell polarity events that form the mating projection, only a subset of these polarity components also function in cell fusion. *FIG1* and *FIG4* are both required for mating projection polarization, whereas only *FIG1* has a role in cell fusion. A recent study has also found that many general polarity components (e.g., Spa2p, Pea2p, Rvs161p, and Bni1p) are required for cell fusion, whereas another (Bem1p) is not (Dorer et al., 1997). Perhaps fusion-specific polarity components recruit and localize cell signaling components (i.e., pheromones, receptors, and transporters), which, in turn, target cell fusion proteins (Brizzio et al., 1996; Elia and Marsh, 1996; Dorer et al., 1997). Alternatively, cell polarity components might directly localize both signaling and cell fusion components to cell-cell contact sites.

Finally, the defects observed in *fig2Δ* zygotes possessing

narrow conjugation bridges reveal a prerequisite of proper conjugation bridge shape for the efficient execution of subsequent events of nuclear fusion and segregation. This requirement further emphasizes the importance of components that regulate the spatial control of mating projection morphogenesis, which, in turn, determines the shape of the conjugation bridge. Since the mating defect of *fig2Δ* strains is normally revealed only by quantitative mating assays and low temperature conditions (conditions not commonly used in genetic screens), it will be interesting to examine mutants in other cell wall components for similar morphological phenotypes.

### ***Fig1p Is a Novel Transmembrane Protein That Functions in Cell Polarization and Fusion***

A number of lines of evidence suggest that Fig1p functions in organization of polarized growth sites during mating. Analysis of the mating morphology of *fig1Δ* mutant cells indicates a role for Fig1p in cell polarization. *fig1Δ* mutants are also defective in cell fusion, which depends upon pheromone signaling and actin-interacting proteins (Brizio et al., 1996; Elia and Marsh, 1996; Dorer et al., 1997). Fig1p could participate in pheromone receptor-directed or cell fusion-targeted polarity functions in a number of different ways. Fig1p might directly or indirectly associate with known components of signaling or fusion complexes located at growth sites initially established by activated pheromone receptors (Madden and Snyder, 1992; Valtz et al., 1995). Alternatively, Fig1p might act by controlling ion flux (see below), which, in turn, affects organization of the actin cytoskeleton. Finally, *fig1Δ* mutants share many properties (e.g., cold sensitivity, EGTA supersensitivity, bilateral cell fusion defects) with mutants defective in *FUS1*, which encodes a type I transmembrane protein (McCaffrey et al., 1987; Trueheart et al., 1987; Elion et al., 1995). Thus, Fig1p and Fus1p may function in the same pathway(s).

The Fig1p is a predicted 4 TM domain-containing protein, and localization of a Fig1::β-gal fusion protein shows that it is likely to reside in the plasma membrane within close proximity to other membrane-associated polarity and cell fusion components, such as the Ste2p and Ste3p transmembrane pheromone receptors, the G-protein subunits, and Fus1p (for review see Sprague and Thorner, 1992). Fig1p also possesses similarities to the mammalian 4 TM superfamily of proteins. Members of this superfamily have been implicated in cell polarity functions in the mammalian immune system (Wright and Tomlinson, 1994). Some of these proteins have been shown to act as effector molecules, coupling G-proteins to their cognate receptors (Wright and Tomlinson, 1994). Fig1p may act in a similar manner by helping recruit general polarity components to sites of activated G-proteins (Leeuw et al., 1995; Madden and Snyder, 1992; Valtz et al., 1995).

Features of the Fig1p sequence suggest it may act as an ion transporter or channel. The presence of charged amino acids at conserved locations within their transmembrane segments has led to speculation that 4 TM superfamily proteins may function as ion transporters (Wright and Tomlinson, 1994). A second 4 TM superfamily of genes, the connexins, also possess such charged domains within their transmembrane segments (Goodenough et al., 1996).

Connexins and ductins, a structurally related group of proteins, function as ion transporters at gap junctions, which are sites of cell-cell contact and communication in higher eukaryotes (Finbow et al., 1994; Goodenough et al., 1996; Bryant, 1997). Fig1p contains charged residues within two predicted transmembrane segments and mating of *fig1Δ* mutants is supersensitive to the addition of EGTA, a chelator of calcium ions. The quantitative mating defect of *fig1Δ* mutants is also rescued by Ca<sup>2+</sup> supplementation of the medium (Erdman, S., unpublished data). It is known that yeast cells exposed to mating pheromone undergo a large calcium influx (Ohsumi and Anraku, 1985). Thus, Fig1p might serve a role in mediating or coupling this ion influx to the activity of other morphogenetic proteins (e.g., Cdc24p; Miyamoto et al., 1987). Although the exact mechanism of its function in mating cell polarization and fusion is not known, Fig1p represents the first component specific to mating cells involved in both these processes. Further study of Fig1p will likely yield significant insights into the nature of the link between cell polarization and fusion during mating.

### ***Fig2p Is a Putative GPI-anchored Cell Surface Protein That Affects Cell Adhesion and Shape***

The sequence of Fig2p predicts it to be an extensively glycosylated protein that is GPI-anchored to the cell surface. The protein is also rich in serine and threonine, similar to many cell surface proteins of yeast (Klis, 1994; Cid et al., 1995). These properties suggest that Fig2p, like other pheromone-regulated cell wall components such as chitin synthase I and a subunit of 1,3-β-D-glucan synthase (encoded by *CHS1* and *FKS2*, respectively), probably function to provide structural support to the newly deposited cell wall of the growing mating projection (Appeltauer and Achstetter, 1989; Mazur et al., 1995).

The role of Fig2p in mating cells provides insights into how cell surface components are coupled to polarized growth processes in the underlying cell cortex and how these components affect cell-cell communication events. Loss of Fig2p function removes a component of the cell wall and produces enhanced apical growth of the mating projection. Thus, disruptions in extracellular components can influence the spatial program of polarized growth in the underlying cell cortex. Perhaps the absence of Fig2p activates a checkpoint monitoring projection growth, analogous to that described for bud morphogenesis (Lew and Reed, 1995). Loss of Fig2p function also causes a novel mating phenotype of hyperagglutination and increased mating efficiency at 30°C under liquid mating conditions. Two hypotheses to account for these effects are either that the absence of Fig2p alters cell wall structure such that agglutinins become more exposed on the cell surface, increasing their effectiveness, or that the pool of GPI anchors or pathway components attaching them to these proteins is limiting so that the absence of one (Fig2p) increases the number of other proteins (e.g., Aga1p or Aga1p) receiving anchors.

Despite their increased efficiency of mating at 30°C, *fig2Δ* mutants are still cold sensitive for mating (18-fold reduced relative to wild-type cells). These mutants also hyperagglutinate during mating at 16°C, indicating their mating defect lies in a cellular process other than agglutination. A striking property of *fig2Δ* mutant cells is their narrow mating

projections relative to wild-type cells, and consequently, an unusually narrow conjugation bridge formed between mating cells. Presumably this long and narrow bridge impedes the movement(s) of nuclei within the zygote. The nuclear movements involved in migration and segregation are dependent upon microtubules making contact with appropriate cortical sites; these sites may be less accessible in *fig2Δ* zygotes (Palmer et al., 1992; Farkasovsky and Kuntzel, 1995). Taken together, these phenotypes of *fig2Δ* zygotes reveal a requirement for proper mating projection shape (and thus fusion bridge shape) for the normal execution of later steps of mating, including nuclear migration and segregation.

### ***Fig4p* Belongs to a Gene Family Whose Members Possess Homology to *Sac1p* and Regulate Actin-dependent Processes**

Like *fig1Δ* mutants, *fig4Δ* mutants are also impaired in mating cell morphogenesis. Fig4p displays extensive sequence similarity to the yeast Sac1p. Mutations in *SAC1* alter actin cytoskeletal and secretory pathway dynamics and cause auxotrophy for inositol (Whitters et al., 1993). Loss of Sac1p function suppresses growth defects caused by certain conditional actin mutations and bypasses secretory defects imposed by mutations in the *SEC14* gene (Cleves et al., 1989). These effects in *sac1Δ* mutants are thought to be the result of altered levels of phosphatidylinositol derivatives, which, in turn, may influence the activity of actin regulatory proteins responsive to inositol triphosphate (InsP<sub>3</sub>) (Whitters et al., 1993; De Camilli et al., 1996). Thus, one potential role for Fig4p in pheromone-induced morphogenesis is in the regulation of effector molecules of the actin cytoskeleton. Such a role for Fig4p is supported by the observation that the distribution of actin in mating projection tips of *fig4Δ* cells is usually dispersed and less intense relative to that in wild-type cells.

Although both proteins play roles in actin-dependent processes, an important issue that remains is whether Fig4p is performing Sac1p-related functions in mating cells or carries out a novel function. At least some conservation of biological activity exists between the two diverged proteins, since multiple copies of *FIG4* are capable of suppressing some phenotypes of a *sac1Δ* mutant (Kearns et al., 1997; Gedvilaite, A., and V. Bankiatis, personal communication). Although Fig4p does not appear to be present in vegetative cells, Sac1p is likely to still be present in *fig4Δ* cells during mating, and may, thus, functionally overlap with Fig4p under these circumstances. We are currently examining the mating properties of *sac1Δ* mutants and *fig4Δ sac1Δ* mutants to address this issue.

Fig4p belongs to a growing family of proteins whose members contain a Sac1p homology domain; based on sequence comparisons this family is composed of several distinct groups (this study; Majerus, 1996). Two Sac1p family members, a human and a *C. elegans* protein, display the highest identity to Fig4p and are likely to be orthologues. Other mammalian members of the Sac1p family have been found to localize to neuronal synapses, which are highly polarized structures (McPherson et al., 1996). These proteins are thought to participate in the actin-dependent endocytosis of membranes from the nerve terminus (De

Camilli et al., 1996). The activity performed by the Sac1p homology domain in any of these proteins remains undetermined. Further study of Fig4p and the family of Sac1p-related proteins should yield important insights into the functions of a large family of proteins that are conserved throughout eukaryotes and play key roles in cell polarity.

### ***KAR5/FIG3* Encodes a Pheromone-regulated Protein Functioning in Nuclear Fusion**

Mutations in *KAR5/FIG3* display the strongest quantitative mating defect of the four genes characterized in this study. This defect was also distinct from those of *fig1Δ*, *fig2Δ*, and *fig4Δ* in that a large number of small and irregularly shaped colonies were generated from the *kar5Δ/fig3Δ* × *kar5Δ/fig3Δ* bilateral matings. These small colonies contain unstable heterokaryons that arise through failures in nuclear fusion. This observation is consistent with the finding that *FIG3* corresponds to the *KAR5* gene (Beh et al., 1997). *KAR5* was identified in a screen for bilateral mating mutants (Kurihara et al., 1994).

The biochemical activity of Kar5p/Fig3p during nuclear fusion is not known. Kar5p contains extended coiled-coil regions, suggesting it either associates with itself or another protein to function in nuclear membrane fusion. Since many structural proteins such as intermediate filaments contain large coiled-coil segments (Steinert and Roop, 1988), Kar5p may play some structural role during nuclear fusion. Kar5p might act in conjunction with the previously described *KAR2/BiP* gene product, which is also involved in nuclear fusion and has mutant phenotypes very similar to *kar5* (Rose et al., 1989). Like Kar2p/BiP, an epitope-tagged Kar5p localizes in an endoplasmic reticulum-like pattern in yeast (Erdman, S., and M. Snyder, unpublished data). Unlike *KAR5*, *KAR2/BiP* is not induced by pheromone (Rose et al., 1989). The process of nuclear membrane fusion, however, displays a requirement for pheromone stimulation (Rose et al., 1986). Kar5p may thus represent the component of the process of nuclear membrane fusion that confers its pheromone requirement.

### **Expression-based Screens and the Identification of Gene Function**

Although many pheromone-induced genes were identified in this screen, mating phenotypes were not observed for most of the insertion mutant strains. A number of recently described pheromone-regulated components incur only subtle defects upon loss of function (Konopka, 1993; Iida et al., 1994; Gammie et al., 1995; Konopka et al., 1995). Additionally, mutations in many of the genes characterized in this study (e.g., *FIG1*, *FIG2*, and *FIG4*) caused relatively mild quantitative mating defects while producing significant morphological defects. Thus, the failure to identify requirements for the other genes tested in our study through measurements of mating efficiency and halo assays of pheromone sensitivity may not be surprising. The functions performed by many of these genes may also be partially or completely overlapped by other genes within the pheromone response pathway or in related parallel pathways that function in mating-specific processes. Identification of such redundant genes by expression-based

methods, nonetheless, provides a valuable first step in the determination of the function of these genes. Further analysis of many of these types of genes will be necessary to obtain a complete understanding of the components and mechanisms that function in yeast mating.

We are grateful to F. Cross for the *MAT $\alpha$*  plasmid and B. Andrews for the *sst2* strains. We thank A. Gedviliate and V. Bankaitis; and C. Beh and M. Rose for communication of results before publication. The technical support of A. Sheehan and especially L. Umansky is gratefully acknowledged. B. Piekos provided expert assistance with electron microscopic techniques. We thank Y. Barral, B. Manning, P. Ross-Macdonald, and S. Vidan for critical comments on the manuscript and members of the Snyder lab for useful discussions. S. Minehart prepared the in-frame *QOR1:: $\beta$ -gal* fusion.

S. Erdman was supported by an American Cancer Society Postdoctoral Fellowship. This research was supported by National Institutes of Health grants (HD32637 and GM36494).

Received for publication 14 August 1997 and in revised form 14 November 1997.

*Note Added in Proof.* The molecular characterization of *KAR5* has recently been reported: Beh, C., V. Brizzio, and M.D. Rose. 1997. *KAR5* encodes a novel pheromone-inducible protein required for homotypic nuclear fusion. *J. Cell Biol.* 139:1063–1076.

## References

Altschul, S.F., W. Gish, W. Miller, E.W. Meyers, and D.J. Lipman. 1990. Basic local alignment search tool. *J. Mol. Biol.* 215:403–410.

Appeltauer, U., and T. Achstetter. 1989. Hormone-induced expression of the *CHS1* gene from *Saccharomyces cerevisiae*. *Eur. J. Biochem.* 181:243–247.

Atcheson, C.L., B. DiDomenico, S. Frackman, R.E. Esposito, and R.T. Elder. 1987. Isolation, DNA sequence, and regulation of a meiosis-specific eukaryotic recombination gene. *Proc. Natl. Acad. Sci. USA.* 84:8035–8039.

Bachmair, A., D. Finley, and A. Varshavsky. 1992. In vivo half-life of a protein is a function of its amino-terminal residue. *Science.* 234:179–186.

Baudin, A., O. Ozier-Kalogeropoulos, A. Denouel, F. Lacroute, and C. Cullin. 1993. A simple and efficient method for direct gene deletion in *Saccharomyces cerevisiae*. *Nucl. Acids Res.* 21:3329–3330.

Boeke, J.D., and S.B. Sandmeyer. 1991. Yeast Transposable Elements. In *The Molecular and Cellular Biology of the Yeast Saccharomyces: Genome Dynamics, Protein Synthesis, and Energetics*. J.R. Broach, J.R. Pringle, and E.W. Jones, editors. Cold Spring Harbor Laboratories, Cold Spring Harbor, NY. 193–262.

Brewster, J., T. de Valoir, N. Dwyer, E. Winter, and M. Gustin. 1993. An osmosensing signal transduction pathway in yeast. *Science.* 259:1760–1763.

Brill, J., E. Elion, and G. Fink. 1994. A role for autophosphorylation revealed by activated alleles of *FUS3*, the yeast MAP kinase homolog. *Mol. Biol. Cell.* 5:297–312.

Brizzio, V., A.E. Gammie, G. Nijbroek, S. Michaelis, and M.D. Rose. 1996. Cell fusion during yeast mating requires high levels of  $\alpha$ -factor mating pheromone. *J. Cell Biol.* 135:1727–1739.

Bryant, P. 1997. Junction genetics. *Dev. Genet.* 20:75–90.

Burns, N., B. Grimwade, P.B. Ross-Macdonald, E.-Y. Choi, K. Finberg, G.S. Roeder, and M. Snyder. 1994. Large-scale characterization of gene expression, protein localization and gene disruption in *Saccharomyces cerevisiae*. *Genes Dev.* 8:1087–1105.

Burns, N., P. Ross-Macdonald, G.S. Roeder, and M. Snyder. 1996. Generation, screening and analysis of *lacZ* fusions in yeast. *Microb. Genome Meth.* 61–79.

Byers, B., and L. Goetsch. 1975. Behavior of the spindle plaques in the cell cycle and conjugation of *Saccharomyces cerevisiae*. *J. Bacteriol.* 124:511–523.

Chang, F., and I. Herskowitz. 1990. Identification of a gene necessary for cell cycle arrest by a negative growth factor of yeast: *FAR1* is an inhibitor of a G1 cyclin, *CLN2*. *Cell.* 63:999–1011.

Chang, T.H., and J. Abelson. 1990. Identification of a putative amidase gene in the yeast *Saccharomyces cerevisiae*. *Nucl. Acids Res.* 18:7180.

Chenevert, J., N. Valtz, and I. Herskowitz. 1994. Identification of genes required for normal pheromone-induced cell polarization in *Saccharomyces cerevisiae*. *Genetics.* 136:1287–1297.

Choi, K., B. Satterberg, D. Lyons, and E. Elion. 1994. *Ste5* tethers multiple protein kinases in the MAP kinase cascade required for mating in *S. cerevisiae*. *Cell.* 78:499–512.

Cid, V., A. Duran, F. del Rey, M. Snyder, C. Nombela, and M. Sanchez. 1995. Molecular basis of cell integrity and morphogenesis in *Saccharomyces cerevisiae*. *Microbiol. Rev.* 59:345–386.

Cleves, A.E., P.J. Novick, and V.A. Bankaitis. 1989. Mutations in the *SAC1*

gene suppress defects in yeast Golgi and yeast actin function. *J. Cell Biol.* 109:2939–2950.

Company, M., C. Adler, and B. Errede. 1988. Identification of a Ty1 regulatory sequence responsive to *STE7* and *STE12*. *Mol. Cell Biol.* 8:2545–2554.

Cross, F., L.H. Hartwell, C. Jackson, and J.B. Konopka. 1988. Conjugation in *Saccharomyces cerevisiae*. *Annu. Rev. Cell Biol.* 4:429–457.

Crouzet, M., M. Urdaci, L. Dulau, and M. Aigle. 1991. Yeast mutant affected for viability upon nutrient starvation: characterization and cloning of the *RVS161* gene. *Yeast.* 7:727–743.

David, C., M. Solimena, and P. De Camilli. 1994. Autoimmunity in stiff-Man syndrome with breast cancer is targeted to the C-terminal region of human amphiphysin, a protein similar to the yeast proteins, *Rvs167* and *Rvs161*. *FEBS (Fed. Eur. Biochem. Soc.) Lett.* 351:73–79.

De Camilli, P., S. Emr, P. McPherson, and P. Novick. 1996. Phosphoinositides as regulators in membrane traffic. *Science.* 271:1533–1539.

Devereaux, J., P. Haerberli, and O. Smithies. 1984. A comprehensive set of sequence analysis programs for the VAX. *Nucl. Acids Res.* 12:387–395.

Dietzel, C., and J. Kurjan. 1987. The yeast *SCG1* gene: a G  $\alpha$ -like protein implicated in the  $\alpha$ - and  $\alpha$ -factor response pathway. *Cell.* 50:1001–1010.

Dorer, R., C. Boone, T. Kimbrough, J. Kim, and L.H. Hartwell. 1997. Genetic analysis of default mating behavior in *Saccharomyces cerevisiae*. *Genetics.* 146:39–55.

Dorer, R., P.M. Pryciak and L.H. Hartwell. 1995. *Saccharomyces cerevisiae* cells execute a default pathway to select a mate in the absence of pheromone gradients. *J. Cell Biol.* 131:845–861.

Elia, L., and L. Marsh. 1996. Role of the ABC transporter *Ste6* in cell fusion during yeast conjugation. *J. Cell Biol.* 135:741–751.

Elion, E.A., J. Trueheart, and G.R. Fink. 1995. *Fus2* localizes near the site of cell fusion and is required for both cell fusion and nuclear alignment during zygote formation. *J. Cell Biol.* 130:1283–1296.

Errede, B., and G. Ammerer. 1989. *STE12*, a protein involved in cell-type specific transcription and signal transduction in yeast is part of protein-DNA complexes. *Genes Dev.* 3:1349–1361.

Farkasovsky, M., and H. Kuntzel. 1995. Yeast *Num1p* associates with the mother cell cortex during S/G2 phase and affects microtubular functions. *J. Cell Biol.* 131:1003–1014.

Finbow, M., M. Harrison, and P. Jones. 1994. Ductin-a proton pump component, a gap junction channel and a neurotransmitter release channel. *Bioessays.* 17:247–254.

Gammie, A.E., L.J. Kurihara, R.B. Vallee, and M.D. Rose. 1995. *DNM1*, a dynamin-related gene, participates in endosomal trafficking in yeast. *J. Cell Biol.* 130:553–566.

Gehring, S., and M. Snyder. 1990. The *SPA2* gene of *Saccharomyces cerevisiae* is important for pheromone-induced morphogenesis and efficient mating. *J. Cell Biol.* 111:1451–1464.

Genbauffe, F.S., and T.G. Cooper. 1986. Induction and repression of the urea amidolyase gene in *Saccharomyces cerevisiae*. *Mol. Cell Biol.* 6:3954–3964.

Gimeno, C.J. 1994. Characterization of *Saccharomyces cerevisiae* pseudohyphal development. Ph.D. thesis. Massachusetts Institute of Technology, Cambridge, MA.

Gimeno, C.J., and G.R. Fink. 1994. Induction of pseudohyphal growth by overexpression of *PHD1*, a *Saccharomyces cerevisiae* gene related to transcriptional regulators of fungal development. *Mol. Cell Biol.* 14:2100–2112.

Gimeno, C.J., P.O. Ljungdahl, C.A. Styles, and G.R. Fink. 1992. Unipolar cell divisions in the yeast *S. cerevisiae* lead to filamentous growth: regulation by starvation and *RAS*. *Cell.* 68:1077–1090.

Goodenough, D., J. Golinger, and D. Paul. 1996. Connexins, connexons, and intercellular communication. *Annu. Rev. Biochem.* 65:475–502.

Hall, J., V. Cherkasova, E. Elion, M. Gustin, and E. Winter. 1996. The osmoregulatory pathway represses mating pathway activity in *Saccharomyces cerevisiae*: isolation of a *FUS3* mutant that is insensitive to the repression mechanism. *Mol. Cell Biol.* 16:6715–6723.

Herskowitz, I. 1995. MAP kinase pathways in yeast: for mating and more. *Cell.* 80:187–197.

Herskowitz, I., H.-O. Park, S. Sanders, N. Valtz, and M. Peter. 1995. Programming of cell polarity in budding yeast by endogenous and exogenous signals. *Cold Spring Harbor Symp. Quant. Biol.*

Herskowitz, I., J. Rine, and J. Strathern. 1992. Mating-type Determination and Interconversion. In *The Molecular and Cellular Biology of the Yeast Saccharomyces*: Vol. 2, Gene Expression. E.W. Jones, J.R. Pringle, and J.R. Broach, editors. Cold Spring Harbor Press, Plainview, NY. 583–656.

Hiltunen, J. K., B. Wenzel, A. Beyer, R. Erdmann, A. Fossa, and W. H. Kunau. 1992. Peroxisomal multifunctional beta-oxidation protein of *Saccharomyces cerevisiae*. Molecular analysis of the *Fox2* gene and gene product. *J. Biol. Chem.* 267:6646–6653.

Iida, H., H. Nakamura, T. Ono, M. S. Okumura, and Y. Anraku. 1994. *MID1*, a novel *Saccharomyces cerevisiae* gene encoding a plasma membrane protein, is required for  $Ca^{2+}$  influx and mating. *Mol. Cell Biol.* 14:8259–8271.

Jackson, C.L., and L.H. Hartwell. 1990. Courtship in *Saccharomyces cerevisiae*: an early cell-cell interaction during mating. *Mol. Cell Biol.* 10:2202–2213.

Jackson, C.L., J.B. Konopka, and L.H. Hartwell. 1991. *S. cerevisiae*  $\alpha$ -pheromone receptors activate a novel signal transduction pathway for mating partner discrimination. *Cell.* 67:389–402.

Jauniaux, J.C., and M. Grenson. 1990. *GAP1*, the general amino acid permease gene of *Saccharomyces cerevisiae*. Nucleotide sequence, protein similarity

- with the other bakers yeast amino acid permeases, and nitrogen catabolite repression. *Eur. J. Biochem.* 190:39–44.
- Johnston, M., and M. Carlson. 1992. Regulation of Carbon and Phosphate Utilization. In *The Molecular Biology of the Yeast Saccharomyces*. J.R. Broach, J.R. Pringle, and E.W. Jones, editors. Cold Spring Harbor Laboratory, Cold Spring Harbor, NY. 193–282.
- Kearns, B., T. McGee, P. Mayinger, A. Gedvilaite, S. Phillips, S. Kagiwada, and V. Bankaitis. 1997. Essential role for diacylglycerol in protein transport from the yeast Golgi complex. *Nature*. 387:101–105.
- Keeney, S., C. Giroux, and N. Kleckner. 1997. Meiosis-specific DNA double-strand breaks are catalyzed by Spo11, a member of a widely conserved protein family. *Cell*. 88:375–384.
- Klis, F.M. 1994. Cell wall assembly in yeast. *Yeast*. 10:851–869.
- Konopka, J.B. 1993. AFR1 acts in conjunction with the  $\alpha$ -factor receptor to promote morphogenesis and adaptation. *Mol. Cell Biol.* 13:6876–6888.
- Konopka, J.B., C. DeMattei, and C. Davis. 1995. AFR1 promotes polarized apical morphogenesis in *Saccharomyces cerevisiae*. *Mol. Cell Biol.* 15:723–730.
- Konopka, J.B., D.D. Jenness, and L.H. Hartwell. 1988. The C-terminus of the *S. cerevisiae*  $\alpha$ -pheromone receptor mediates an adaptive response to pheromone. *Cell*. 54:609–620.
- Kron, S.J., C.A. Styles, and G.R. Fink. 1994. Symmetric cell division in pseudohyphae of the yeast *Saccharomyces cerevisiae*. *Mol. Biol. Cell*. 5:1003–1022.
- Kronstad, J.W., J.A. Holly, and V.L. MacKay. 1987. A yeast operator overlaps an upstream activation site. *Cell*. 50:369–377.
- Kunau, W.H., and A. Hartig. 1992. Peroxisome biogenesis in *Saccharomyces cerevisiae*. *Antonie Leeuwenhoek*. 62:63–78.
- Kurihara, L.J., C.T. Beh, M. Latterich, R. Schekman, and M.D. Rose. 1994. Nuclear congression and membrane fusion: two distinct events in the yeast karyogamy pathway. *J. Cell Biol.* 126:911–923.
- Kurihara, L.J., B.G. Stewart, A.E. Gammie, and M.D. Rose. 1996. Kar4p, a karyogamy-specific component of the yeast pheromone response pathway. *Mol. Cell Biol.* 16:3990–4002.
- Kurjan, J. 1993. The pheromone response pathway in *Saccharomyces cerevisiae*. *Annu. Rev. Genet.* 27:147–179.
- Leeuw, T., A. Fourest-Lieuvin, C. Wu, J. Chenevert, K. Clark, M. Whiteway, D.Y. Thomas, and E. Leberer. 1995. Pheromone response in yeast: association of Bem1p with proteins of the MAP kinase cascade and actin. *Science*. 270:1210–1213.
- Lew, D.J., and S.I. Reed. 1995. A cell cycle checkpoint monitors cell morphogenesis in budding yeast. *J. Cell Biol.* 129:739–749.
- Liu, H., C.A. Styles, and G.R. Fink. 1993. Elements of the yeast pheromone response pathway required for filamentous growth of diploids. *Science*. 262:1741–1744.
- Ljungdahl, P.O., C.J. Gimeno, C.A. Styles, and G.R. Fink. 1992. SHR3: a novel component of the secretory pathway specifically required for localization of amino acid permeases in yeast. *Cell*. 71:463–478.
- Madden, K., and M. Snyder. 1992. Specification of sites of polarized growth in *Saccharomyces cerevisiae* and the influence of external factors on site selection. *Mol. Biol. Cell*. 3:1025–1035.
- Madhani, H., and G.R. Fink. 1997. Combinatorial control required for the specificity of yeast MAPK signaling. *Science*. 275:1314–1317.
- Magasanik, B. 1992. Regulation of Nitrogen Utilization. In *The Molecular and Cellular Biology of the Yeast Saccharomyces*. J.R. Broach, J.R. Pringle, and E.W. Jones, editors. Cold Spring Harbor Press, Cold Spring Harbor, NY. 283–318.
- Majerus, P.W. 1996. Inositols do it all. *Genes Dev.* 10:1051–1053.
- Mazur, P., N. Morin, W. Baginsky, M. El-Sherbeini, J. Clemas, J. Nielsen, and F. Foor. 1995. Differential expression and function of two homologous subunits of yeast 1,3- $\beta$ -D-glucan synthase. *Mol. Cell Biol.* 15:5671–5681.
- McCaffrey, G., F.J. Clay, K. Kelsay, and G.F. Sprague, Jr. 1987. Identification and regulation of a gene required for cell fusion during mating of the yeast *Saccharomyces cerevisiae*. *Mol. Cell Biol.* 7:2680–2690.
- McPherson, P.S., E. Garcia, V. Slepnev, C. David, X. Zhang, D. Grabs, W. Sosin, R. Bauerfeind, Y. Nemoto, and P.D. Camilli. 1996. A presynaptic inositol-5-phosphatase. *Nature*. 379:353–357.
- Measday, V., L. Moore, J. Ogas, M. Tyers, and B. Andrews. 1994. The PCL2 (ORFD)-PHO85 cyclin dependent kinase complex: a cell cycle regulator in yeast. *Science*. 266:1391–1395.
- Mewes, H. et al. 1997. The yeast genome directory. *Nature*. 387 (Suppl.):7–8.
- Michaelis, S. 1993. STE6, the yeast  $\alpha$ -factor transporter. *Semin. Cell Biol.* 4:17–27.
- Miyajima, I., M. Nakafuku, N. Nakayama, C. Brenner, A. Miyajima, K. Kaibuchi, K. Arai, Y. Kaziro, and K. Matsumoto. 1987. GPA1, a haploid-specific essential gene, encodes a yeast homolog of mammalian G protein which may be involved in mating factor signal transduction. *Cell*. 50:1011–1019.
- Miyamoto, S., Y. Ohya, Y. Ohsumi, and Y. Anraku. 1987. Nucleotide sequence of the *CLS4 (CDC24)* gene of *Saccharomyces cerevisiae*. *Gene*. 54:125–132.
- Mizuta, K., T. Hashimoto, and E. Otaka. 1995. The evolutionary relationships between homologs of ribosomal YL8 protein and YL8-like proteins. *Curr. Genet.* 28:19–25.
- Munn, A., B. Stevenson, M. Geli, and H. Riezman. 1995. *end5*, *end6*, and *end7*: mutations that cause actin delocalization and block the internalization step of endocytosis in *Saccharomyces cerevisiae*. *Mol. Biol. Cell*. 6:1721–1742.
- Novick, P., B.C. Osmond, and D. Botstein. 1989. Suppressors of yeast actin mutations. *Genetics*. 121:659–674.
- Ogawa, N., K. Noguchi, H. Sawai, Y. Yamashita, C. Yompakdee, and Y. Oshima. 1995. Functional domains of Pho81p, an inhibitor of Pho85p protein kinase, in the transduction pathway of Pi signals in *Saccharomyces cerevisiae*. *Mol. Cell Biol.* 15:997–1004.
- Ohsumi, Y., and Y. Anraku. 1985. Specific induction of  $\text{Ca}^{2+}$  transport activity in MATa cells of *Saccharomyces cerevisiae* by a mating pheromone,  $\alpha$ -factor. *J. Biol. Chem.* 260:10482–10486.
- Olson, M.V. 1991. Genome Structure and Organization in *Saccharomyces cerevisiae*. In *The Molecular and Cellular Biology of the Yeast Saccharomyces: Genome Dynamics, Protein Synthesis, and Energetics*. J.R. Broach, J.R. Pringle, and E.W. Jones, editors. Cold Spring Harbor Laboratories, Cold Spring Harbor, NY. 1–39.
- Page, B.D., and M. Snyder. 1992. CIK1: a developmentally regulated spindle pole body-associated protein important for microtubule functions in *Saccharomyces cerevisiae*. *Genes Dev.* 6:1414–1429.
- Palmer, R.E., D.S. Sullivan, T. Huffaker, and D. Koshland. 1992. Role of astral microtubules and actin in spindle orientation and migration in the budding yeast, *Saccharomyces cerevisiae*. *J. Cell Biol.* 119:583–593.
- Price, C., K. Nasmyth, and T. Schuster. 1991. A general approach to the isolation of cell cycle-regulated genes in the budding yeast, *Saccharomyces cerevisiae*. *J. Mol. Biol.* 218:543–556.
- Pringle, J., A.E.M. Adams, D.G. Drubin, and B.K. Haarer. 1991. Immunofluorescence Methods for Yeast. In *Yeast Genetics and Molecular Biology*. C. Guthrie and G.R. Fink, editors. Academic Press, NY. 565–601.
- Pringle, J., E. Bi, H. Harkins, J. Zahner, C. Devirgilio, J. Chant, K. Corado, and H. Fares. 1995. Establishment of cell polarity in yeast. *Cold Spring Harbor Symp. Quant. Biol.* 60:729–744.
- Reiser, J., A. Muheim, M. Hardegger, G. Frank, and A. Fiechter. 1994. Aryl-alcohol dehydrogenase from the white-rot fungus *Phanerochaete chrysosporium*. Gene cloning, sequence analysis, expression, and purification of the recombinant enzyme. *J. Biol. Chem.* 269:28152–28159.
- Roberts, R., and G.R. Fink. 1994. Elements of a single MAP kinase cascade in *Saccharomyces cerevisiae* mediate two developmental programs in the same cell type: mating and invasive growth. *Genes Dev.* 8:2974–2985.
- Robinson, L., E. Hubbard, P. Graves, A. DePaoli-Roach, P. Roach, C. Kung, D. Haas, C. Hagedorn, M. Goebel, M. Culbertson et al. 1992. Yeast casein kinase I homologues: an essential gene pair. *Proc. Natl. Acad. Sci. USA*. 89:28–32.
- Roemer, T., L. Vallier, and M. Snyder. 1996. Selection of polarized growth sites in yeast. *Trends Cell Biol.* 6:434–441.
- Rose, M.D., and L. Marsh. 1997. The Pathway of Cell and Nuclear Fusion during Mating in *S. cerevisiae*. *Cell Cycle and Cell Biology*. Vol. 3. J.R. Pringle, J.R. Broach, and E.W. Jones, editors. Cold Spring Harbor Laboratory Press, Plainview, NY. 583–656.
- Rose, M.D., L.M. Misra, and J.P. Vogel. 1989. KAR2, a karyogamy gene, is the yeast homolog of the mammalian BiP/GRP78 gene. *Cell*. 57:1211–1221.
- Rose, M.D., B.R. Price, and G.R. Fink. 1986. *Saccharomyces cerevisiae* nuclear fusion requires prior activation by  $\alpha$  factor. *Mol. Cell Biol.* 6:3490–3497.
- Rose, M.D., F. Winston, and P. Hieter. 1990. *Methods in Yeast Genetics: A Laboratory Course Manual*. Cold Spring Harbor Laboratories, Cold Spring Harbor, NY. 198 pp.
- Sambrook, J., E.F. Fritsch, and T. Maniatis. 1989. *Molecular Cloning: A Laboratory Manual*. Cold Spring Harbor Laboratory, Cold Spring Harbor, NY.
- Schiebert, E.M., M.E. Egan, T.H. Hwang, S.B. Fulmer, S.S. Allen, G.R. Cutting, and W.B. Guggino. 1995. CFTR regulates outwardly rectifying chloride channels through an autocrine mechanism involving ATP. *Cell*. 81:1063–1073.
- Segall, J.E. 1993. Polarization of yeast cells in spatial gradients of  $\alpha$ -factor. *Proc. Natl. Acad. Sci. USA*. 90:8332–8336.
- Sherman, F., G.R. Fink, and J. Hicks. 1986. *Methods in Yeast Genetics*. Cold Spring Harbor Laboratories, Cold Spring Harbor, NY.
- Sikorski, R., and P. Hieter. 1989. A system of shuttle vectors and yeast host strains designed for efficient manipulation of DNA in *Saccharomyces cerevisiae*. *Genetics*. 122:19–27.
- Sprague, G.F., Jr., and J. Thorner. 1992. Pheromone Response and Signal Transduction during the Mating Process of *Saccharomyces cerevisiae*. In *The Molecular Biology of the Yeast Saccharomyces*. J.R. Broach, J.R. Pringle, and E.W. Jones, editors. Cold Spring Harbor Laboratory, Cold Spring Harbor, NY. 657–744.
- Sprague, G.F., Jr. 1991. Assay of yeast mating reaction. *Meth. Enzymol.* 194:77–93.
- Stanbrough, M., and B. Magasanik. 1995. Transcriptional and posttranslational regulation of the general amino acid permease of *Saccharomyces cerevisiae*. *Proc. Natl. Acad. Sci. USA*. 177:94–102.
- Steinert, P.M., and R. Roop. 1988. The molecular and cellular biology of intermediate filaments. *Annu. Rev. Biochem.* 57:593–625.
- Stetler, G.L., and J. Thorner. 1984. Molecular cloning of hormone-responsive genes from the yeast *Saccharomyces cerevisiae*. *Proc. Natl. Acad. Sci. USA*. 81:1144–1148.
- Stevenson, B., B. Ferguson, C. De Virgilio, E. Bi, J. Pringle, G. Ammerer, and G.F. Sprague Jr. 1995. Mutation of RGA1, which encodes a putative GTPase-activating protein for the polarity-establishment protein Cdc42p, activates the pheromone-response pathway in the yeast *Saccharomyces cerevisiae*. *Genes Dev.* 9:2949–2963.
- Timblin, B., K.K. Tatchell, and L.W. Bergman. 1996. Deletion of the gene encoding the cyclin-dependent protein kinase Pho85 alters glycogen metabolism in *Saccharomyces cerevisiae*. *Genetics*. 143:57–66.
- Trueheart, J., J.D. Boeke, and G.R. Fink. 1987. Two genes required for cell fu-

- sion during yeast conjugation: evidence for a pheromone-induced surface protein. *Mol. Cell. Biol.* 7:2316–2328.
- Trueheart, J., and G.R. Fink. 1989. The yeast cell fusion protein FUS1 is O-glycosylated and spans the plasma membrane. *Proc. Natl. Acad. Sci. USA.* 86: 9916–9920.
- Valenzuela, P., G.I. Bell, A. Venegas, E.T. Sewell, F.R. Masiarz, L.J. Degenaro, F. Weinberg, and W.J. Rutter. 1977. Ribosomal rna genes of *Saccharomyces cerevisiae*: ii. Physical map and nucleotide sequence of the 5S ribosomal rna gene and adjacent intergenic regions. *J. Biol. Chem.* 252:8126–8135.
- Valtz, N., M. Peter, and I. Herskowitz. 1995. *FAR1* is required for oriented polarization of yeast cells in response to mating pheromones. *J. Cell Biol.* 131: 863–873.
- Van Arsdell, S.W., G.L. Stetler, and J. Thorner. 1987. The yeast repeated element sigma contains a hormone-inducible promoter. *Mol. Cell Biol.* 7:749–759.
- Velculescu, V.E., L. Zhang, W. Zhou, J. Vogelstein, M.A. Basrai, D.E. Bassett Jr., P. Hieter, B. Vogelstein, and K.W. Kinzler. 1997. Characterization of the yeast transcriptome. *Cell.* 88:243–251.
- Voytas, D.F., and J.D. Boeke. 1992. Yeast retrotransposon revealed. *Nature.* 358:717.
- Wang, X., M.F. Hoekstra, A.J. DeMaggio, N. Dhillon, A. Vancura, J. Kuret, G.C. Johnston, and R.A. Singer. 1996. Prenylated isoforms of yeast casein kinase I, including the novel Yck3p, suppress the gcs1 blockage of cell proliferation from stationary phase. *Mol. Cell. Biol.* 16:5375–5385.
- Weiner, B., and N. Kleckner. 1994. Chromosome pairing via multiple interstitial interactions before and during meiosis in yeast. *Cell.* 77:977–991.
- Whitters, E.A., A.E. Cleves, T.P. McGee, H.B. Skinner, and V.A. Bankaitis. 1993. SAC1p is an integral membrane protein that influences the cellular requirement for phospholipid transfer protein function and inositol in yeast. *J. Cell Biol.* 122:79–94.
- Wieland, J., A.M. Nitsche, J. Strayle, H. Steiner, and H.K. Rudolph. 1995. The PMR2 gene cluster encodes functionally distinct isoforms of a putative Na<sup>+</sup> pump in the yeast plasma membrane. *EMBO (Eur. Mol. Biol. Organ.) J.* 14: 3870–3882.
- Wright, M.D., and M.G. Tomlinson. 1994. The ins and outs of the transmembrane 4 superfamily. *Immunol. Today.* 15:588–594.
- Xie, K., E. Lambie, and M. Snyder. 1993. Nuclear dot antigens may specify transcriptional domains in the nucleus. *Mol. Cell. Biol.* 13:6170–6179.